Effect of Visual Feedback on Behavioral Control and Functional Activity During Bilateral Hand Movement

Jing Guo
Xi'an Jiaotong University School of Life Science and Technology https://orcid.org/0000-0002-3990-7684

Long Li
Xi'an Jiaotong University School of Life Science and Technology

Yang Zheng
Xi'an Jiaotong University School of Life Science and Technology

Ain Quratul
Xi'an Jiaotong University School of Life Science and Technology

Tian Liu
Xi'an Jiaotong University School of Life Science and Technology

Jue Wang (juewang_xjtu@126.com)
Xi'an Jiaotong University School of Life Science and Technology

---

Research

Keywords: Visual Feedback, Theta band, Alpha band, Force Accuracy, Efficiency

Posted Date: December 4th, 2020

DOI: https://doi.org/10.21203/rs.3.rs-118986/v1

Effect of visual feedback on behavioral control and functional activity during bilateral hand movement

Jing Guo[1,2,3], Long Li[1,2,3], Yang Zheng[4], Ain Quratul[1,2,3], Tian Liu*[1,2,3], Jue Wang*[1,2,3]

1. The Key Laboratory of Biomedical Information Engineering of Ministry of Education, Institute of Health and Rehabilitation Science, School of Life Science and Technology, Xi'an Jiaotong University, Xi'an, Shaanxi, 710049, People's Republic of China.

2. National Engineering Research Center for Healthcare Devices. Guangzhou, Guangdong, 510500, People's Republic of China.

3. The Key Laboratory of Neuro-informatics & Rehabilitation Engineering of Ministry of Civil Affairs, Xi'an, Shaanxi, 710049, People's Republic of China.

4. State Key Laboratory for Manufacturing Systems Engineering, School of Mechanical Engineering, Xi'an Jiaotong University, Xi'an, Shaanxi, 710049, People's Republic of China

Address Correspondence to Tian Liu and Jue Wang. The key Laboratory of Biomedical Information Engineering of Ministry of Education. The key Laboratory of Neuro-informatics & Rehabilitation Engineering of Minnistry of Civil Affairs, Xi'an Jiaotong University, Institute of Biomedical Engineering, School of Life Science and Technology, Xi'an 710049, People's Republic of China.

Electronic mails: tianliu@xjtu.edu.cn, juewang_xjtu@126.com

Key words: Visual Feedback; Theta band; Alpha band; Force Accuracy; Efficiency

Abstract

Background: Previous researches state vision as vital source of information for movement control and more precisely for accurate hand movement. Further, fine bimanual motor activity may be associated to various oscillatory activities within distinct brain areas and inter-hemispheric interactions. However, neural coordination among the distinct brain areas responsible to enhance motor accuracy is still not adequate.

Methods: In the current study we investigated task-dependent modulation by simultaneously measuring high time resolution electroencephalogram (EEG), electromyogram (EMG) and force along with bi-maual and uni-manual motor tasks. The errors were controlled using visual feedback. In order to complete the uni-manual tasks, subject was asked to grip the strain gauge using index finger and thumb of right hand thereby exerting force on connected visual feedback system. Whereas the bi-manual task involved finger abduction of left index finger in two contractions along with visual feedback system and at the same time the right hand gripped using definite force on two conditions that whether visual feedback existed or not for right hand.

Results: Primarily, the existence of visual feedback for right hand significantly decreased brain network global and local efficiency in theta and alpha band when compared with the elimination of visual feedback.

Conclusions: Brain network activity in theta and alpha band coordinate to facilitate fine hand movement. The findings may provide a new neurological insight on virtual reality auxiliary equipment and subjects with neurological disorders that cause movement errors requiring accuracy motor training.

1. Background

Fine motor control requires two types of feedback including intrinsic and extrinsic feedback; extrinsic feedback is primarily the visual feedback (Desmurget, et al., 2000, Miall, 1996). It is an established fact by a range of studies that visual feedback can improve various motor behaviors, such as force control, upper limb movement and handwriting (Jacobs, et al., 1992, Seidler, et al., 2001, Sosnoff and Newell, 2005). Especially, visual feedback can potentially improve fine hand movement requiring a great deal of accuracy (Elliott and Allard, 1985, Lebar, et al., 2015). Moreover, visual feedback has been shown to play an important role in visuomotor processing. For instance, in a bimanual precise force griping task, for left hand without visual feedback, beta band corticomuscular coherence was only found over the contralateral primary motor cortex (MI) instead of contralateral MI and supplementary motor area (SMA) region in right hand with visual feedback (Chen, et al., 2013). Recent studies have shown that visual feedback can increase the complexity of the electroencephalogram during visuomotor task (Shafer, et al., 2019). Although many researchers suggested that visual information could make a difference on the motor performance and neural process, however, the topological properties of the brain network connection in this process are still not well understood.

There is abundant evidence across many studies showing that functional processing of information input was associated with different band-specific neural oscillations in movement (Bauer, et al., 2014, Lebar, et al., 2017a, Pelt, et al., 2016). Theta band was related to the movement observation, cognitive control processes and strategy adjustment of action in multiple brain areas (Cohen, 2011, 2014, Duprez, et al., 2020, Yordanova, et al., 2020). Alpha band serves as a local marker for the degree of excitability of the somatosensory and visual cortices, with a lower alpha

power being related to higher activity level (Lebar, et al., 2017b). Beta oscillations are obvious during steady states when subjects perform visually guided motor control activities (Mehrkanoon, et al., 2014). The processing or somatosensory integration is related to beta desynchronization (Lebar, et al., 2017b). Gamma oscillations contribute to a higher order of sensory information integration to deal with unimodal and multimodal sensory binding and encode stimuli of different sensory modalities (Krebber, et al., 2015). These researches suggested that neural oscillations in different bands may process distinct functions. Thus, we infer that which band or co-frequency oscillations play a significant role in visuo-motor and somatosensory input during steady-hold hand movement.

The modulation of visual input might be involved in several brain areas. For instance, visual information would project primary processing in the occipital pool (Livingstone and Hubel, 1988). Recognition and identification of the intricate visual process were involved in temporal region (Ariel and Itzhak, 2012, Newsome and Paré, 1988) whereas the spatial representation and multisensory integration were related to posterior parietal region (Andersen, 2011). Visually-guided motor activity involved multiple brain areas that coordinate to facilitate movement performance. Dipietro et al. found that frontoparietal network was related with visually guided upper limb movements (Dipietro, et al., 2014) . Besides, corpus callosum connects the cerebral hemispheres on both sides at the anatomical level and it mainly participates in the exchange of information across the two hemispheres for functions including organization of bimanual movement, integrate feeling and vision (Netz and Ziemann, 1995). The studies discussed above state that online visually-motor correction of bilateral hand movement involved multiple areas where distributed different functional cortex. Thus, we analyzed underlying neurophysiological process from the perspective of the whole brain network based on graph-theory during visuomotor task. Bimanual motions are important for humans in daily

life, since a lot of tasks require cooperative bimanual hands to achieve the goal. Thus, studying the network characteristic during bimanual task is significant.

Different types of neural processing were reflected through different carrier frequency, embody the impact on frequency dependent network during visually-guide sustained contraction. Thus, the purpose of this research was to study the impact of visual feedback on the brain network through different frequency. We performed bilateral and unilateral hand movement and controlled the movement errors using visual feedback. Unique force was exerted from right hand with visual feedback in the uni-manual task while in the bimanual tasks, conditions were divided into four tasks based on whether visual feedback existed for the right hand and two contraction levels of the left-hand muscles. Based on graph theory analysis, network efficiency was used to capture the efficiency of information transfer and the assemble characteristics underlying the observed functional network.

2. Methods

2.1 Subjects

A total number of 22 healthy subjects with normal or corrected-to-normal vision were involved in this research. All participants were fully informed and consent forms were obtained prior to the experiment. The experiment was approved by ethical committee of Xi'an Jiaotong University. The healthy subjects were recruited from Xi'an Jiaotong University. Participants with history of psychiatric disorders and those having any physical illness that can affect hand movement were excluded from the study. All participants were measured by the Edinburgh Handedness Inventory (Oldfield, 1971). The average laterality score was 95.23 ± 4.85 for 21 right-handed subjects. The score was -88 for the left-hand subject. In this study, in order to remove the possible effect of

111 handedness, a left-hand subject was excluded from the subsequent analysis. The average age of the
112 participants was 21 years and the age ranged between 18-23 years.

113 **2.2 Experimental design and task**

114 The baseline task was a right hand uni-manual precision grip using index finger and the thumb
115 pinching a strain gauge to exert a 2-N constant force connected to visual feedback system. In the
116 bimanual task, the subjects were instructed to abduct the index finger of their left hand to exert two
117 types of force involving 5% maximum voluntary contraction (MVC) and 50% MVC by squeezing
118 another strain gauge. Visual feedback of the exerted force and target force of bimanual hands were
119 showed on the 19" monitor placed approximately 100cm in front of subject (**Figure 1**). In a half of
120 the task, the visual feedback will disappear and the participant needs to maintain exerted force in the
121 maintenance phase. Therefore, based on the contraction level of left hand muscles and whether visual
122 feedback exist or not for the right hand, four combined conditions were obtained, naming
123 'RF-L5', 'RF-L50', 'R-L5', 'R-L50', where 'RF' meant retained visual feedback of right hand, 'R'
124 meant visual feedback of right hand was removed. 'L5' meant contraction force of left hand was 5%
125 MVC, 'L50' meant contraction force of left hand was 50% MVC. Simultaneously, the unimanual
126 task was named as 'RF-L0'.

127 Duration of each trail was 6 seconds (s), during the first 2s the subject adjusted applied force to
128 target force and during the last 4s the subjects maintain the target force with or without visual
129 feedback during the steady-hold period for right hand. At the end of each trail, the subjects rested for
130 nearly 2s. During the resting time, visual feedback of both hands was eliminated before the next trial
131 was conducted. The subjects were instructed to conduct one uni-manual task and seven bi-manual
132 tasks, one subject conducted three bi-manual tasks. The unimanual task block contained 60 trials and

133 every bimanual block contained 40 trials. In each bimanual block, each of the 4 conditions contained
134 10 trials that were distributed randomly.

135 Participants adjusted the exerted force through the vision feedback on screen. The screen
136 contained two pairs of rings that included solid circle and hollow circle. The subject should move
137 solid circle into the hollow circle. The upper part displayed a pair of circles. According to the
138 distance from the hollow circle, it was divided into 50% MVC and 5% MVC for left-hand muscle.
139 The bottom of the screen displayed a pair if circle showing performance of the right hand. **Figure 2**
140 showed the schematic of experiment process.

141 **2.3 Data acquisition and preprocessing**

142 The subjects were sitting in a dim and electromagnetic shielded room. SynAmps2 system
143 (Neuroscan, El Paso, TX, USA) recorded high-resolution EEG and EMG data. EEG signal was
144 acquired from 60 mounted Ag/AgCl channels that were positioned according to the international
145 10-20 system. The signal was referenced with respect to the vertex. Electrooculography (EOG) was
146 monitored by four separated channels that were positioned around the eye. Two electrodes were used
147 for EMG that was positioned at the right and left first dorsal interosseous (rFDI and lFDI) muscle.
148 The ground electrode of EEG and EMG was positioned on the midline of the scalp at the level of
149 prefrontal cortex. EEG and EMG signals were amplified (EMG: band pass, 5–100 Hz; EEG: band
150 pass, DC to 100 Hz) and were sampled at 1000 Hz. During the recording session, the impedance of
151 each channel was maintained below 5 kΩ. Two force sensors were used to record the force exert by
152 the participants simultaneously. The force signal was digitized at 200Hz.

153 A block diagram of EEG, EMG and force signal processing and analysis pipeline is shown in
154 **Figure 3**. First, a zero-phase finite impulse response (FIR) filter was applied with a high-pass at 0.1

Hz and a low-pass at 45 Hz. Electrodes with artifacts were recounted with topographic interpolated using surrounding channels. Raw EMG signal was high-pass filtered at 5Hz. The filtered EMG signals were rectified by taking the absolute value. Second, the informax independent component analysis (ICA) algorithm was applied to decompose the EEG data into independent components (ICs) using the EEGLAB toolbox (Bell and Sejnowski, 1995, Delorme and Makeig, 2014). Then, ADJUST plug-in was applied in the ICs to distinguish non-brain components and to remove the irrelevant EEG components in EEGLAB (Mognon, et al., 2011). This plug-in can distinguish the irrelevant EEG components with joint use of spatial and temporal features. The criteria for rejecting the component also included component scalp map, activity power spectrum and activity time course (Delorme and Makeig, 2014). The artifact components including horizontal eye movement, vertical eye movement, blink, discontinuities and muscle activity were discarded. Third, EEG, EMG and force signal of epoch 8s was extracted which included 1s before movement and 1s post movement. EEG were baseline-corrected using the entire epoch to remove the linear trends. Finally, epochs with the amplitude of steady-hold of right hand above $\pm$50% target force were rejected. The discarding epochs were 10.0 ± 7.6 for the subjects. All preprocessing was conducted using EEGLAB (14_1_1b) and MATLAB 2018b (The Math Works Inc.). Then, the surface segmented EEG was transformed into the reference-free current source density (CSD) estimates implementing scalp surface Laplacian using a spherical spline algorithm (Perrin, et al., 1989). Scalp surface Laplacian is a fine approximate evaluation to be proportional to the dura potential (Nunez, 1987), and can remove nearly all volume conduction errors (Nunez, et al., 1997). The spherical spline algorithm was conducted in the CSD toolbox (version 1.1) (Kayser and Tenke, 2006a, b) .

2.4 Data analysis

177 The first step for EMG analysis was to calculate the activation level of each muscle in the time
178 domain, we analyzed raw EMG signal in every task to get EMG activity. The process is as follows:
179 (1) The raw EMG signals were off-line high-pass filtered at 10 Hz. (2) The filtered EMG signals
180 were rectified by taking the absolute value. (3) The rectified data was low-pass filter at 5 Hz. (4) The
181 filtered EMG signals were baseline-corrected using the entire epoch to remove the linear trends. (5)
182 To obtain the mean EMG activity for all subject, the processed data was averaged across all trials and
183 subjects in each condition (Chen, et al., 2013). In the following, we use the term 'EMG activity' for
184 this preprocessed EMG. After processing, CSD, EMG, and force data within steady-hold periods
185 during which the accuracy was obtained around a target were used for further analysis.

186 **2.4.1 Brain network formation**

187 In this study, we consider each CSD signal as a representation of the underlying brain function.
188 The spectral coherence is estimated from each pair of the electrodes. Each electrode of the CSD
189 signal is considered as a vertex in the formed brain functional network. The connection strength is
190 assigned to each edge by its corresponding spectral coherence value to from a weighted graph. To
191 formally define the above described procedure, we denote m_x and m_y as the analytic signals of
192 EEG electrodes X and Y, the vertical bar surrounding signal X and Y means the magnitude of them,
193 ϕ_{xy} means the phase angle difference between signal X and Y, t means trials points. Thus, the
194 spectral coherence between two channels could be found as following.

195 $$C_{xy}(f) = \left| n^{-1} \sum_{t=1}^{n} \left| m_{tx} \right\| m_{ty} \left| e^{i\phi_{txy}} \right| \right|^2 \quad (1)$$

196 $$S_{xy}(f) = \frac{C_{xy}(f)}{(n^{-1} \sum_{t=1}^{n} \left| m_{tx} \right|^2)(n^{-1} \sum_{t=1}^{n} \left| m_{ty} \right|^2)} \quad (2)$$

197 Where sum and n^{-1} indicates the average over magnitude-modulated phase value. The

198 obtained spectral coherence is normalized to lie in the range of 0 to 1. With the estimated
199 connectivity measure, we have constructed the adjacency matrix $\mathbf{A}$ of the proposed brain network.
200 The adjacency matrix $\mathbf{A}$ is given as:

201
$$\mathbf{A}=\begin{bmatrix} A_{1,1} & A_{1,2} & K & A_{1,M} \\ M & M & M & M \\ A_{M,1} & A_{M,2} & \Lambda & A_{M,M} \end{bmatrix} \tag{3}$$

202 Where M is the total number of electrodes available and each element in $\mathbf{A}$, denoted as $A_{x,y}$,
203 represents the connection strength between the x-th and y-th channel (Bullmore and Sporns, 2009).
204 The value of $A_{x,y}$ is given as:

205
$$A_{x,y} \equiv \bar{S}_{xy} \tag{4}$$

206 Where $\bar{S}_{xy}$ denotes the average spectral coherence value at given frequency band, frequency
207 band were divided into theta band (4~7Hz) , alpha band (8~13Hz) , beta band (14~30Hz) and gamma
208 band (31~45Hz) .

209 **2.4.2 Network analysis**

210 With the obtained task-related brain network, efficiency was employed to study its topographic
211 properties. The graph measure collapsed the overall topological features of a given brain functional
212 network into a single measurement. Therefore, it facilitates the comparison of the obtained brain
213 network between different tasks in normal. The weighted graph version of the two graph metrics,
214 namely, local efficiency (Eloc) and global efficiency (Eglob) were selected due to their novelty in the
215 brain functional network analysis (Wang, et al., 2010). To mathematically define these graph
216 measures, we first denote $k_i = \sum_{j \in G} A_{i,j}$ as the degree of *i*-th node, where G is the set of all
217 possible vertex of the obtained brain functional network, and n is the number of nodes,
218 $d_{ij}^{w} = \sum_{a_{uv} \in gi \leftrightarrow j}^{w} f(A_{uv})$, where f is a map (e.g., an inverse) from weight to length and $g_{i \leftrightarrow j}^{w}$ is the

219 shortest weighted path between *i* and *j*, *w* means weighted graph, a_{uv} is the state of the connection
220 between *u* and *v*.

221 The global efficiency was developed to overcome the difficulties that inherited in the
222 characteristic path length. It differs with the characteristic path length by using the reciprocal value
223 of the shortest path length. Global efficiency supports the efficient transfer of parallel information at
224 a relatively low cost. Global efficiency is a reliable measure to study the function integration. It is
225 defined as：

226 $$\mathrm{Eglob}^{w} = \frac{1}{n}\sum_{i\in G}\frac{1}{n-1}\sum_{j\in G, j\neq i}\frac{1}{d_{ij}^{w}} \tag{5}$$

227 The local efficiency represents the fault tolerance of the network. Local efficiency of a weighted
228 graph represents the function separation. It is defined as follow:

229 $$\mathrm{Eloc}^{w} = \frac{1}{2}\sum_{i\in G}\frac{1}{k_i(k_i-1)}\sum_{j,h\in G, j\neq i}(A_{ij}A_{ih}[d_{jh}(G_i)]^{-1})^{1/3} \tag{6}$$

230 Where G_i denotes the number of neighbors of node *i*. For details on the graph measures,
231 please refer to (Rubinov and Sporns, 2010).

232 So as to capture the graph measures among these networks, the networks need to be properly
233 pruned so that the false connections can be reduced, while keeping the threshold to trim the
234 connection with sub-threshold strength. After selecting the sparsity, the graph measures were
235 computed and the sparsity level was selected by using the following procedure. First, the graph
236 sparsity was defined as the fraction of preserved strongest connection to the total number of all
237 possible connections in the obtained network. Then, band-wise matrices were thresholded to retain
238 between 10%-50% of the largest coherence value. The sparsity of 10% insured that mean degree
239 $K \geq 2 \times \log(V)$, V=60 nodes, this boundary ensured the graphs were estimable (Albrecht, et al., 2016,

Chennu, et al., 2014). Besides, above the sparsity of 50%, the networks tend to be random and less small-world increasingly (Chennu, et al., 2014). At each value of the sparsity, the global and local efficiency were calculated across the thresholded and weighted matrices for individual network in each band and condition using Brain Connectivity Toolbox in MATLAB (Rubinov and Sporns, 2010). All network results reported are average of sparsity range 10-50% (41 values, 1% steps) in this study.

2.4.3 Force accuracy, EMG steadiness and EMG activity

Force accuracy was measured by root mean square error (RMSE) (Wang, et al., 2018), which was defined as following equation:

$$\mathrm{RMSE}_{\mathrm{N}} = \left(\sum \frac{(s - f_i)^2}{m-1}\right)^{\frac{1}{2}} \tag{7}$$

N is the n-th data epoch, s is the target force, f_i is i-th force sample, m is the number of sampling point.

We determined the coefficient of variation of EMG as measures of EMG steadiness (EMG_CV), EMG_CV was defined as follow (Ahamed, et al., 2016, Graziadio, et al., 2010, Long, et al., 2016):

$$\mathrm{EMG\_CV}_{\mathrm{N}} = 1 - \frac{SD(\mathrm{EMG}_{\mathrm{N\_Rectified}})}{mean(\mathrm{EMG}_{\mathrm{N\_Rectified}})} \tag{8}$$

N_Rectified is the n-th rectified EMG epoch. *SD* denotes standard error of the n-th rectified EMG epoch, *mean* shows the average value of the n-th rectified EMG epoch and $\mathrm{EMG\_CV}_{\mathrm{N}}$ is the EMG_CV value of n-th rectified EMG epoch.

2.4.4 Statistical analysis

In this study, we used two steps of statistical analysis to test the hypotheses. First, we used RF-L0, RF-L5 and RF-L50 to test how the left-hand muscle at different level influence the force accuracy, EMG steadiness, global and local efficiency using repeated-measure ANOVA. Second, we

used two-factor within-subject repeated measure ANOVA analysis between task RF-L5, R-L5, RF-L50 and R-L50 with 21 subjects to test the effect of the contraction level (5% and 50% of MVC) of the left hand and visual feedback for right hand on the accuracy of the exert force, EMG steadiness, the local efficiency, global efficiency of network during steady-hold period. Post hoc test was corrected by the Holm-Bonferroni measure. Significance was set at $p<0.05$. Group data are presented as $M \pm SD$. Statistical analysis was carried by using Statistical Product and Service Solutions (IBM SPSS Statistics, version 22).

3. Results

3.1 Behavior performance

Figure 4 shows the average behavior results for every subject performing the ramp-hold precision grip task during RF-L0, RF-L5, R-L5, RF-L50, R-L50. **Figure 4 (a)** and **Figure 4 (b)** shows the time course of average forces and average EMG activities of both hands for each condition respectively. **Figure 4 (a)** represent all trajectories rang around the target force along the whole time period, whereas **Figure 4 (b)** shows the mean EMG activity within a specific range, these results represented that subjects met the experiment requirements under every task.

3.2 Force RMSE and EMG_CV

Force RMSE was average across all subjects for the right hand (**Figure 5**). To verify whether different task conditions had significant influence on right-hand muscle activities, we used the two-steps statistical analysis. The mean force RMSE was 0.0760 ± 0.0347 for task RF-L0, 0.1017 ± 0.0352 for task RF-L5, 0.1660 ± 0.0740 for task R-L5, 0.1161 ± 0.0414 for task RF-L50 and 0.1512 ± 0.0542 for task R-L50. In the first-step statistical analysis, the results of ANOVA showed that the force RMSE differed between task RF-L0, RF-L5 and RF-L50 (F=22.466, df=2, p=0.009).

Further post hoc analysis showed significant differences between task RF-L0 and RF-L5 (p<0.001), RF-L0 and RF-L50 (p<0.001). No significant difference was found between task RF-L5 and RF-L50 (p=0.141) (**Table 1**). In the second step of the statistical analysis, a two-factor within-subject repeated measures ANOVA was used to analyze the influence of visual feedback and the contraction level of left-hand muscles for right hand on the force RMSE. The ANOVA results showed that the visual feedback significantly influenced the force accuracy (F=38.900, df=1, p<0.001). The contraction level of left-hand muscles had no significant influence on the force accuracy (F<0.001, df=1, p=0.984) (**Table 2**). The interaction of visual feedback × contraction level of left-hand muscle was significant (F=11.859, df=1, p=0.003). Post hoc test showed that force RMSE increased significantly during task RF-L50 compared with that during RF-L5 (p=0.047), however, the difference was not significant between task R-L5 and task R-L50 (p=0.193). Meanwhile, force RMSE increased during task R-L5 compared with task RF-L5 (p<0.001) and during task R-L50 compared with task RF-L50 (p<0.001).

Table1: The result statistical analysis for tasks RF-L0, RF-L5 and RF-L50

	F	*df*	*p*	*p*(1,2)	*p*(1,3)	*p*(2,3)
RMSE	22.466	2	**0.009**	**<0.001**	**<0.001**	0.141
EMG_CV	7.397	1.389	**0.006**	0.127	**0.012**	0.103
Theta_Eglob	7.607	1.057	**0.011**	**0.029**	**0.040**	1.000
Theta_Eloc	7.704	1.128	**0.009**	**0.023**	**0.040**	1.000
Alpha_Eglob	12.847	1.020	**0.002**	**0.008**	**0.004**	**0.037**
Alpha_Eloc	13.100	1.041	**0.001**	**0.007**	**0.004**	0.186
Beta_Eglob	6.139	1.047	**0.021**	0.056	0.075	1.000
Beta_Eloc	3.445	1.069	0.075	0.173	0.315	0.441
Gamma_Eglob	8.746	1.061	**0.007**	**0.019**	**0.026**	0.712
Gamma_Eloc	4.296	1.111	**0.046**	0.121	0.184	0.621

Note: *p* (1,2) means the statistical significance between RF-L0 and RF-L5 , *p* (1,3) means the statistical significance between RF-L0 and RF-L50, *p* (2,3) means the statistical significance between RF-L5 and RF-L50.

Table2: The result statistical analysis for tasks RF-L5, R-L5, RF-50 and R-L50

	Left contraction			Visual feedback			Left contraction*Visual feedback		
	df	*F*	*p*	*df*	*F*	*p*	*df*	*F*	*p*
RMSE	1	<0.001	0.984	1	38.900	**<0.001**	1	11.859	**0.003**
EMG_CV	1	8.184	**0.010**	1	<0.001	0.993	1	1.705	0.206
Theta_Eglob	1	1.621	0.218	1	7.686	**0.012**	1	0.493	0.491
Theta_Eloc	1	0.962	0.338	1	5.511	**0.029**	1	0.739	0.400
Alpha_Eglob	1	13.008	**0.002**	1	33.990	**<0.001**	1	3.771	0.066
Alpha_Eloc	1	11.636	**0.003**	1	54.614	**<0.001**	1	3.018	0.098
Beta_Eglob	1	0.341	0.566	1	1.023	0.324	1	0.905	0.353
Beta_Eloc	1	0.953	0.341	1	0.693	0.415	1	1.702	0.207
Gamma_Eglob	1	1.615	0.218	1	0.952	0.341	1	0.463	0.504
Gamma_Eloc	1	0.685	0.418	1	0.972	0.336	1	1.666	0.212

EMG_CV were averaged across all 21 subjects for rFDI during each task (**Figure 6**). The mean EMG_CV was 0.1012 ± 0.0553 for task RF-L0, 0.1196 ± 0.0704 for task RF-L5, 0.1181 ± 0.0721 for task R-L5, 0.1294 ± 0.0618 for task RF-L50 and 0.1309 ± 0.0637 for task R-L50. In the first-step statistical analysis, the results of ANOVA showed that the EMG_CV differed between task RF-L0, RF-L5 and RF-L50 (F=7.397, df=1.389, p=0.006). Further post hoc analysis showed no significant difference was found between task RF-L0 and RF-L5 (p=0.127), RF-L5 and RF-L50 (p=0.103), and significant difference between RF-L0 and RF-L50 (p=0.012). In the second step of the statistical analysis, a two-factor within-subject repeated measures ANOVA was used to analyze the influence of the contraction level of left-hand muscles and visual feedback for right hand on the EMG steadiness. The ANOVA results showed that the visual feedback does not significantly influenced the EMG steadiness (F<0.001, df=1, p=0.993). The contraction level of left-hand muscles had significant influence on the EMG steadiness (F=8.184, df=1, p=0.010). The interaction effect between visual feedback × contraction level of left-hand muscles had no significant difference on EMG_CV (F=1.705, df=1, p=0.206) (**Table 2**).

3.3 Graph theory-based measure

Global and local efficiency were averaged across all 21 subjects in theta (4-7Hz), alpha

316 (8-13Hz), beta (14-30Hz) and gamma (31-45Hz) band during each task (**Figure 7**). Further, we
317 applied the statistical analysis to the following steps. The purpose of statistical analysis for graph
318 theory-based measures was to determine whether significant differences occurred in the network of
319 the whole cortical oscillatory in different motion conditions. In the first step of the statistical analysis,
320 the global efficiency and local efficiency of the whole brain were averaged across all subjects for
321 tasks RF-L0, RF-L5 and RF-L50. The ANOVA results showed that global efficiency had significant
322 difference in theta band (F=7.607, df=1.057, p=0.011), alpha band (F=12.847, df=1.020, p=0.002),
323 beta band (F=6.139, df=1.047, p=0.021) and gamma band (F=8.746, df=1.061, p=0.007) between
324 tasks RF-L0, RF-L5 and RF-L50. Besides, the ANOVA results showed that local efficiency had no
325 significant difference in beta band (F=3.445, df=1.069, p=0.075) between tasks RF-L0, RF-L5 and
326 RF-L50, rather than in theta band (F=7.704, df=1.128, p=0.009), alpha band (F=13.100, df=1.041,
327 p=0.001) and gamma band (F=4.296, df=1.111, p=0.046). Further post hoc test demonstrated the
328 statistical analysis of global efficiency between tasks RF-L0 and RF-L5 (p=0.029, p=0.008, p=0.056,
329 p=0.019), RF-L0 and RF-L50 (p=0.040, p=0.004, p=0.075, p=0.026), RF-L5 and RF-L50 (p=1.000,
330 p=0.037, p=1.000, p=0.712) in theta, alpha, beta and gamma band respectively. Besides, post hoc test
331 demonstrated the statistical analysis of local efficiency between tasks RF-L0 and RF-L5 (p=0.023,
332 p=0.007, p=0.173, p=0.121), RF-L0 and RF-L50 (p=0.040, p=0.004, p=0.315, p=0.184), RF-L5 and
333 RF-L50 (p=1.000, p=0.186, p=0.441, p=0.621) in theta, alpha, beta, and gamma band respectively
334 (**Table 1**).

335 In the second step of the statistical analysis, a two-factor within-subject repeated measures
336 ANOVA was used to analyze the influence of the contraction level of left-hand muscles and visual
337 feedback for right hand on the mean theta, alpha, beta and gamma band. The ANOVA results showed

that only the visual feedback significantly influenced the global efficiency and local efficiency in theta band (F=7.686, df=1, p=0.012), (F=5.511, df=1, p=0.029), alpha band (F=33.990, df=1, p<0.001), (F=54.614, df=1, p<0.001) rather than in beta band (F=1.023, df=1, p=0.324), (F=0.693, df=1, p=0.415) and gamma band (F=0.952, df=1, p=0.341), (F=0.972, df=1, p=0.336). The contraction level of left-hand muscles had no significant influence on the global efficiency and local efficiency in theta (F=1.621, df=1, p=0.218), (F=0.962, df=1, p=0.338), beta (F=0.341, df=1, p=0.566), (F=0.953, df=1, p=0.341) and gamma (F=1.615, df=1, p=0.218), (F=0.685, df=1, p=0.418) rather than in alpha band (F=13.008, df=1, p=0.002), (F=11.636, df=1, p=0.003) (**Table 2**).

The interaction of visual feedback×contraction level of left-hand muscle was not significant on theta global efficiency (F=0.493, df=1, p=0.491), theta local efficiency (F=0.739, df=1, p=0.400), alpha global efficiency (F=3.771, df=1, p=0.066) , alpha local efficiency (F=3.018, df=1, p=0.098), beta global efficiency (F=0.905, df=1, p=0.353), beta local efficiency (F=1.702, df=1, p=0.207) , gamma global efficiency (F=0.463, df=1, p=0.504) and gamma local efficiency (F=1.666, df=1, p=0.212).

4. Discussion

We investigated the influence of manipulating visual feedback and contraction level of one hemisphere hand muscles related to sustain force output, neuromuscular activity and cortical oscillatory processes during voluntary movement of hand. We obtained three new results. First, the elimination of visual feedback for right hand significantly decreased force accuracy in right hand. Second, movement error decreased in unimanual task compared with bimanual task. Besides, EMG_CV decreased in uni-manual task compared with the bimanual task of moderate isometric contraction of left hand muscle. In addition, global and local efficiency of network was larger in

unimanual task compared with bimanual task in the theta and alpha band. Besides, global efficiency of network were larger in unimanual task compared with bimanual task in gamma band. Furthermore, moderate isometric contraction of left hand muscle induced a significant decrease in global efficiency of network in alpha band compared with weak isometric contraction of left hand muscle. Third, the existence of visual feedback resulted in decreased global efficiency and local efficiency of network of theta and alpha band in the whole brain when compared to eliminate visual feedback. These observations were not found in beta and gamma band, suggesting a frequency-dependent nature to the changes in the brain network. These findings indicated that theta and alpha band oscillations coordinate to accurate hand movement.

4.1 Effects of visual feedback on force output and neuromuscular activity

In the current study, visual information was used to manipulate movement accuracy. Compared with the elimination of the visual feedback, the existence of visual feedback increased the force accuracy. Jae W.Chung et al. conducted elbow flexor and extensor neuromuscular activity during ballistic movements, he separated movement error rate using low and high visual gain (Chung, et al., 2017). Compared to the low visual feedback, high visual gain significantly decreased the error and associated with the alpha band, beta band and gamma band desynchronization between parietal and contralateral sensorimotor cortex (Chung, et al., 2017). Bagce HF et al. found that visual feedback enhance performance and may modulate MI excitability in stroke patients during finger flexion or extension (Bagce, et al., 2012). Based on previous studies, we extend the elbow activity or one hand motion into bimanual hand movement to investigate the effect of visual feedback.

We found that movement error of right hand muscle decreased in unimanual task compared with bimanual task. However, no significant difference was found between weak contraction of left hand

and moderate contraction of left hand. Similar results were found in Smits Engelsman BC' study, they found that the error of force increased in the bimanual task compared with unimanual task (Smits-Engelsman, et al., 2004). These results suggested that co-contraction may increase the involvement of the antagonistic muscle, this process could recruit noise, thus, bring about extra movement disturbances.

EMG steadiness is an essential ability for mobility of daily activities. EMG steadiness is caused by several factors such as aging, muscle contraction level and the use of unilateral or bilateral hand (Long, et al., 2016, Tracy and Enoka, 2002, Ushiyama, et al., 2017). In the present study, EMG steadiness was not be influenced by visual feedback of right hand and the contraction level of left hand. The reason could be that the influence of visual feedback and the contraction level of left hand between uni-manual task and bimanual task of weak isometric contraction of left hand muscle on rFDI steadiness are weak when compared with EMG variability. Thus, subtle factors-dependent variables may be submerged in EMG random oscillations. In addition, EMG_CV decreased in uni-manual task compared with the bimanual task of moderate isometric contraction of left hand muscle. However, no significant difference was found between uni-manual task and bimanual task of weak isometric contraction of left hand muscle. The reason was similar with force error that the involvement of the antagonistic muscle may bring about additional motor disturbances in the bimanual task of moderate isometric contraction of left hand muscle.

4.2 Task related neural activity and motor performance

We found that brain network in theta and alpha band had significantly decreased global efficiency and local efficiency with visual feedback, suggesting that theta and alpha band of the brain network bears the load with visual feedback of right hand during steady-hold period. The functional

network has been dynamically reorganized in different tasks, such as visual gain, visual feedback, finger movement and motor learning (Archambault, et al., 2015, Bédard and Sanes, 2014, Mehrkanoon, et al., 2016, Ushiyama, et al., 2017). Network system with a low local efficiency indicates a looser substructure connection of the network. Conversely, when local efficiency is higher, network topology is more robust in local information processing even if existed in inefficient or damaged neurons (Liang, et al., 2010, Yu, et al., 2011). Thus, the obtained results suggest that brain is more sensitive in tasks with visual feedback compared to the tasks without visual feedback. This may be accounted for that network topology of tasks with visual feedback are more complex compared with tasks without visual feedback, which subjects should pay more attention to adapt the external factors in bimanual movement. Global efficiency quantifies the information transferring at a macro-scopic level. A high global efficiency has advantages in minimizing noise, shortening the time delay of signal transfer and increasing the synchronization of network in network system (Wang, et al., 2012). In the current study, significant differences existed in global efficiency in conditions that whether visual feedback existed or not for right hand. Global efficiency of network was associated with widespread cortical regions responsible for visual input. This suggested that neural process may organize sparser neuronal assemblies with visual feedback. Tasks with visual feedback involve feed-forward and feed-backward process to improve fine movement response. In addition, increased visual feedback could add the load of the brain compared with tasks without visual feedback due to attenuated feedback process. Besides, visual feedback participated in the long-distance feedback projections to visual areas from the top areas of the hierarchical model (Clavagnier, et al., 2004), this process could improve the transfer time of information thereby decreasing the efficiency of network. The lower efficiency means the longer transfer and process time. Generally, longer time paid to the

task results better performance and vice versa (Nasir, et al., 2017). These results indicated the complex the tasks were, the greater load of the brain undertake, the greater time of the brain cost, the lower local and global efficiency were. Stanley Matthew L. et al found that local efficiency was significantly decreased in working memory compared with resting state. Global efficiency was decreased relatively when compared with resting state during the working memory tasks, they also found that the better the performance of old subjects were, the lower global efficiency was (Stanley, et al., 2015). Lou W et al. found that the performance was negatively correlated with local efficiency and global efficiency in healthy subjects (Lou, et al., 2015).

4.3 Theta band and visually-guided movement

Theta band has shown been bound up with the sensorimotor integration (Caplan, et al., 2001, Zarka, et al., 2014). Furthermore, theta band serve as the underlying physiological component related to global oscillatory synchronization course connecting multiple brain areas (Zarka, et al., 2014). Rey et al. applied single-neuron and local field potential technology demonstrate that theta locking embodies a global activation in visual recognition task (Rey, et al., 2014). Visual gain regulated theta band desynchroniztion during visually-guided upper limb movement (Chung, et al., 2017). In this study, the novel finding here is that visual feedback modulated global and local efficiency of theta band network, suggesting that the global integration and separation attributes of theta band of the brain network influenced the visual feedback of right hand during steady-hold period.

4.4 Alpha band activity and attentional processing

Alpha band activity was related to attentional process and visually guided motor control. Jinyi Long et al. found that EEG-EEG coherence decreased during bilateral finger movement compared with unilateral task in alpha band, they also found decreased EEG spectral power in alpha band.

448 Their results suggested that alpha band has a role in error corrections and suppressing task-irrelevant
449 activity during hand movements (Long, et al., 2016). Besides, alpha band may contribute to
450 influence the reconstitution of sensory area of brain to conduct information flow and improve
451 performance (Haegens, et al., 2011). On the basis of above appoint, numerous studies on visual tasks
452 have shown that alpha band activity is related to attention orientation (Fu, et al., 2001), visual
453 (Tuladhar, et al., 2007) and somatosensory working-memory performance (Haegens, et al., 2010).
454 Furthermore, decreased alpha oscillatory facilitates neuronal processing (Haegens, et al., 2011).
455 Pfurtscheller et al. reported that event related synchronization or desynchronization express the
456 neurons and inter-neurons activity in the network (Pfurtscheller and Lopes, 1999). Thus, we
457 conclude that the regulation of the global efficiency and local efficiency of brain network in alpha
458 band in the whole brain are associated with good performance with multi-source visual information.

459 **4.5 Effects of the level of isometric contraction on neural activity**

460 In this study, unilateral isometric contraction of right hand muscle induced a significant increase
461 in the global and local efficiency of network in theta, alpha band compared with week (5% of MVC)
462 and moderate (50% of MVC) isometric contraction of left hand muscle, and a significant increase in
463 global efficiency of network in gamma band compared with week (5% of MVC) and moderate (50%
464 of MVC) isometric contraction of left hand muscle. Alpha band serve as a sensitive function in
465 detecting changes during force generation (Abdul-Latif, et al., 2004). Previous studies showed that
466 the EEG-EEG coherence and EEG spectral power decreased during bilateral activity as compare
467 with unilateral force in alpha band (Long, et al., 2016). Besides, intermittent theta burst stimulation
468 to the left dorsal premotor cortex can enhance primary motor cortex excitability during bimanual
469 visuomotor training (Neva, et al., 2015). Gamma band may connect neural cluster that encode

multiple sensory modulation (Lebar, et al., 2017a). In the bilateral task, divided attention may participate in bimanual movement. When unilateral isometric contraction takes place, global and local efficiency increased, because divided attention was limited. When left hand was performing weak and moderate isometric contraction, global and local efficiency decreased, because attention was affected. Besides, this mechanism is sensitive to global efficiency. In this study, we found that weak (5% of MVC) isometric contraction of right hand muscle induced a significant increase in the global efficiency of network in alpha band compared with moderate (50% of MVC) isometric contraction of left hand muscle. Thus, the present study suggests a broad-band network regulation across theta, alpha and gamma band during sustain force output.

There are several limitations in the current analysis. Firstly, the relatively small number of subjects and the epoch number restrict its statistic results in this study. Secondly, the constructed brain functional network considers linear dependency between a pair of electrodes and the obtained connections are directionless. It is impossible to deduce the underlying information propagation in detail. Therefore, we intend to adopt non-linear and directional measure in our future study to delineate the detailed information loop under visually guided hand movement.

5. Conclusions

Our research explores the neurophysiology evidence between brain oscillations network and online visuomotor performance. In this research, movement errors were reduced with visual feedback. Movement error decreased in unimanual task compared with bimanual task. In addition, EMG_CV decreased in uni-manual task compared with the bimanual task that moderate isometric contraction of left hand muscle. Moreover, global and local efficiency of network was larger in unimanual task compared with bimanual task in the theta and alpha band. Besides, global efficiency

of network were larger in unimanual task compared with bimanual task in gamma band. Furthermore, moderate isometric contraction of left hand muscle induced a significant decrease in global efficiency of network in alpha band compared with weak isometric contraction of left hand muscle. We also observed changes in decreased global and local efficiency of network in theta and alpha band in the whole brain with visual feedback, suggesting that specific band suppression of oscillation network occurred in theta and alpha band during steady hold period. Further, we suggest that theta and alpha band synchronous network in the whole brain were associated with attentional allocation and visual information to optimize motor performance for visual information during motor corrections. These findings have a considerable impact on clinical training of virtual reality auxiliary equipment, and provide a new insight on neurological disorders that cause movement errors that are required for accuracy motor training.

Declarations:

Ethics approval and consent to participate:

All participants were fully informed and consent forms were obtained prior to the experiment. The experiment was approved by ethical committee of Xi'an Jiaotong University.

Consent for publication

Not applicable.

Availability of data and materials

The datasets generated and/or analysed during the current study are not publicly available due data privacy but are available from the corresponding author on reasonable request.

Competing interests

514 The authors declare that they have no competing interests.

515 **Funding**

516 The study was financially supported by the National Natural Science Foundation of China
517 (Grant No. U1913216), National Key Research and Development Program of China (Grant
518 No.2017YFB1300303, 2018YFC2002601), Natural Science Foundation of Shaanxi Province (Grant
519 No. 2018JM7080), China Postdoctoral Science Foundation (Grant No. 2018M643672) and
520 Fundamental Research Funds for the Central Universities (Grant No. xjh01219049).

521 **Authors' contributions**

522 JW and YZ design and perform of experiment; JG analyzed data; JG and TL interpreted results
523 of experiment; JG prepared figures; JG drafted manuscript; JG and AQ modified the grammar; JG,
524 TL, LL and JW edited and revised manuscript; JG, TL, and JW approved final version of manuscript.

525 ## Acknowledgments

526 Not applicable.

527 .

528 ## References

529 Abdul-Latif A, Cosic I, Kumar D, Polus B, Pah N and Djuwari D. Eeg coherence changes between
530 right and left motor cortical areas during voluntary muscular contraction. Australas. Phys. Eng. Sci.
531 Med. 27: 11, 2004. https://doi.org/10.1007/BF03178882

532 Ahamed N, Rabbi M, Taha Z, Sundaraj K and Sikandar T. The effects of rest interval on
533 electromyographic signal on upper limb muscle during contraction. Journal 10-13, 2016.
534 https://doi.org/10.1007/978-981-10-3737-5_3

535 Albrecht MA, Roberts G, Price G, Lee J, Iyyalol R and Martin-Iverson MT. The effects of

536 dexamphetamine on the resting-state electroencephalogram and functional connectivity. Hum. Brain
537 Mapp. 37: 570-588, 2016. https://doi.org/10.1002/hbm.23052
538 Andersen RA. Inferior parietal lobule function in spatial perception and visuomotor integration.
539 Compr. Physiol. 483-518, 2011. https://doi.org/10.1002/cphy.cp010512
540 Archambault PS, Ferrari-Toniolo S, Caminiti R and Battaglia-Mayer A. Visually-guided correction
541 of hand reaching movements: The neurophysiological bases in the cerebral cortex. Vision Res. 110:
542 244-256, 2015. https://doi.org/10.1016/j.visres.2014.09.009
543 Ariel T and Itzhak F. Visuomotor coordination and motor representation by human temporal lobe
544 neurons. J. Cognit. Neurosci. 24: 600, 2012. https://doi.org/10.1162/jocn_a_00160
545 Bagce HF, Soha S, Adamovich SV and Eugene T. Visuomotor gain distortion alters online motor
546 performance and enhances primary motor cortex excitability in patients with stroke.
547 Neuromodulation 15: 361-366, 2012. https://doi.org/10.1111/j.1525-1403.2012.00467.x
548 Bauer M, Stenner M-P, Friston KJ and Dolan RJ. Attentional modulation of alpha/beta and gamma
549 oscillations reflect functionally distinct processes. J. Neurosci. 34: 16117-16125, 2014.
550 https://doi.org/10.1523/JNEUROSCI.3474-13.2014
551 Bédard P and Sanes JN. Brain representations for acquiring and recalling visual–motor adaptations.
552 NeuroImage 101: 225-235, 2014. https://doi.org/10.1016/j.neuroimage.2014.07.009
553 Bell AJ and Sejnowski TJ. An information-maximization approach to blind separation and blind
554 deconvolution. Neural Comput. 7: 1129-1159, 1995. https://doi.org/10.1162/neco.1995.7.6.1129
555 Bullmore E and Sporns O. Complex brain networks: Graph theoretical analysis of structural and
556 functional systems. Nat. Rev. Neurosci. 10: 186-198, 2009. https://doi.org/10.1038/nrn2575
557 Caplan JB, Madsen JR, Raghavachari S and Kahana MJ. Distinct patterns of brain oscillations

558 underlie two basic parameters of human maze learning. J. Neurophysiol. 86: 368-380, 2001.
559 https://doi.org/10.1152/jn.2001.86.1.368
560 Chen S, Entakli J, Bonnard M, Berton E and De Graaf JB. Functional corticospinal projections from
561 human supplementary motor area revealed by corticomuscular coherence during precise grip force
562 control. PLoS One 8: e60291, 2013. https://doi.org/10.1371/journal.pone.0060291
563 Chennu S, Finoia P, Kamau E, Allanson J, Williams GB, Monti MM, Noreika V, Arnatkeviciute A,
564 Canales-Johnson A and Olivares F. Spectral signatures of reorganised brain networks in disorders of
565 consciousness. PLoS Comput. Biol. 10: e1003887, 2014.
566 https://doi.org/10.1371/journal.pcbi.1003887
567 Chung JW, Ofori E, Misra G, Hess CW and Vaillancourt DE. Beta-band activity and connectivity in
568 sensorimotor and parietal cortex are important for accurate motor performance. NeuroImage 144:
569 164-173, 2017. https://doi.org/10.1016/j.neuroimage.2016.10.008
570 Clavagnier S, Falchier A and Kennedy H. Long-distance feedback projections to area v1:
571 Implications for multisensory integration, spatial awareness, and visual consciousness. Cogn. Affect.
572 Behav. Ne. 4: 117-126, 2004. https://doi.org/10.3758/CABN.4.2.117
573 Cohen MX. Error-related medial frontal theta activity predicts cingulate-related structural
574 connectivity. NeuroImage 55: 1373-1383, 2011. https://doi.org/10.1016/j.neuroimage.2010.12.072
575 Cohen MX. A neural microcircuit for cognitive conflict detection and signaling. Trends Neurosci. 37:
576 480-490, 2014. https://doi.org/10.1016/j.tins.2014.06.004
577 Delorme A and Makeig S. Eeglab wiki. 2014
578 Desmurget M, Grafton and Scott. Forward modeling allows feedback control for fast reaching
579 movements. Trends Cogn. Sci. 4: 423-431, 2000. https://doi.org/10.1016/S1364-6613(00)01537-0

580 Dipietro L, Poizner H and Krebs HI. Spatiotemporal dynamics of online motor correction processing
581 revealed by high-density electroencephalography. J. Cognit. Neurosci. 26: 1966-1980, 2014.
582 https://doi.org/10.1162/jocn_a_00593
583 Duprez J, Gulbinaite R and Cohen MX. Midfrontal theta phase coordinates behaviorally relevant
584 brain computations during cognitive control. NeuroImage 207: 116340, 2020.
585 https://doi.org/10.1016/j.neuroimage.2019.116340
586 Elliott D and Allard F. The utilization of visual feedback information during rapid pointing
587 movements. Q. J. Exp. Psychol. 37: 407, 1985. https://doi.org/10.1080/14640748508400942
588 Fu K-MG, Foxe JJ, Murray MM, Higgins BA, Javitt DC and Schroeder CE. Attention-dependent
589 suppression of distracter visual input can be cross-modally cued as indexed by anticipatory
590 parieto–occipital alpha-band oscillations. Cognit. Brain Res. 12: 145-152, 2001.
591 https://doi.org/10.1016/S0926-6410(01)00034-9
592 Graziadio S, Basu A, Tomasevic L, Zappasodi F, Tecchio F and Eyre JA. Developmental tuning and
593 decay in senescence of oscillations linking the corticospinal system. J. Neurosci. 30: 3663-3674,
594 2010. https://doi.org/10.1523/JNEUROSCI.5621-09.2010
595 Haegens S, Nácher V, Luna R, Romo R and Jensen O. Alpha-oscillations in the monkey sensorimotor
596 network influence discrimination performance by rhythmical inhibition of neuronal spiking. Proc.
597 Natl. Acad. Sci. U. S. A. 108: 19377-19382, 2011. https://doi.org/10.1073/pnas.1117190108
598 Haegens S, Osipova D, Oostenveld R and Jensen O. Somatosensory working memory performance
599 in humans depends on both engagement and disengagement of regions in a distributed network. Hum.
600 Brain Mapp. 31: 26-35, 2010. https://doi.org/10.1002/hbm.20842
601 Jacobs R, Van SD and Schotte A. The importance of visual feedback on the accuracy of jaw and

finger positioning in man. Arch. Oral Biol. 37: 677-683, 1992. https://doi.org/10.1016/0003-9969(92)90071-F

Kayser J and Tenke CE. Principal components analysis of laplacian waveforms as a generic method for identifying erp generator patterns: I. Evaluation with auditory oddball tasks. Clin. Neurophysiol. 117: 348-368, 2006a. https://doi.org/10.1016/j.clinph.2005.08.034

Kayser J and Tenke CE. Principal components analysis of laplacian waveforms as a generic method for identifying erp generator patterns: Ii. Adequacy of low-density estimates. Clin. Neurophysiol. 117: 369-380, 2006b. https://doi.org/10.1016/j.clinph.2005.08.033

Krebber M, Harwood J, Spitzer B, Keil J and Senkowski D. Visuotactile motion congruence enhances gamma-band activity in visual and somatosensory cortices. NeuroImage 117: 160-169, 2015. https://doi.org/10.1016/j.neuroimage.2015.05.056

Lebar N, Bernier PM, Guillaume A, Mouchnino L and Blouin J. Neural correlates for task-relevant facilitation of visual inputs during visually-guided hand movements. NeuroImage 121: 39-50, 2015. https://doi.org/10.1016/j.neuroimage.2015.07.033

Lebar N, Danna J, Moré S, Mouchnino L and Blouin J. On the neural basis of sensory weighting: Alpha, beta and gamma modulations during complex movements. NeuroImage 150: 200-212, 2017a. https://doi.org/10.1016/j.neuroimage.2017.02.043

Lebar N, Danna J, Moré S, Mouchnino L and Blouin J. On the neural basis of sensory weighting: Alpha, beta and gamma modulations during complex movements. Neuroimage 150: 200, 2017b.

Liang W, Metzak PD, Honer WG and Woodward TS. Impaired efficiency of functional networks underlying episodic memory-for-context in schizophrenia. J. Neurosci. 30: 13171-13179, 2010. https://doi.org/10.1523/JNEUROSCI.3514-10.2010

Livingstone M and Hubel D. Segregation of form, color, movement, and depth: Anatomy, physiology, and perception. Science 240: 740-749, 1988. https://doi.org/10.1126/science.3283936

Long J, Tazoe T, Soteropoulos DS and Perez MA. Interhemispheric connectivity during bimanual isometric force generation. J. Neurophysiol. 115: 1196-1207, 2016. https://doi.org/10.1152/jn.00876.2015

Lou W, Shi L, Wang D, Tam CW, Chu WC, Mok VC, Cheng ST and Lam LC. Decreased activity with increased background network efficiency in amnestic mci during a visuospatial working memory task. Hum. Brain Mapp. 36: 3387-3403, 2015. https://doi.org/10.1002/hbm.22851

Mehrkanoon S, Boonstra TW, Breakspear M, Hinder M and Summers JJ. Upregulation of cortico-cerebellar functional connectivity after motor learning. NeuroImage 128: 252-263, 2016. https://doi.org/10.1016/j.neuroimage.2015.12.052

Mehrkanoon S, Breakspear M and Boonstra TW. The reorganization of corticomuscular coherence during a transition between sensorimotor states. NeuroImage 100: 692-702, 2014. https://doi.org/10.1016/j.neuroimage.2014.06.050

Miall RC. Task-dependent changes in visual feedback control: A frequency analysis of human manual tracking. J. Mot. Behav. 28: 125, 1996. https://doi.org/10.1080/00222895.1996.9941739

Mognon A, Jovicich J, Bruzzone L and Buiatti M. Adjust: An automatic eeg artifact detector based on the joint use of spatial and temporal features. Psychophysiology 48: 229-240, 2011. https://doi.org/10.1111/j.1469-8986.2010.01061.x

Nasir AFAA, Clemente CJ, Wynn ML and Wilson RS. Optimal running speeds when there is a trade-off between speed and the probability of mistakes. Funct. Ecol. 31: 1941-1949, 2017. https://doi.org/10.1111/1365-2435.12902

Netz J and Ziemann UV. Hemispheric asymmetry of transcallosal inhibition in man. Exp. Brain Res. 104: 527-533, 1995. https://doi.org/10.1007/BF00231987

Neva JL, Vesia M, Singh AM and Staines WR. Bilateral primary motor cortex circuitry is modulated due to theta burst stimulation to left dorsal premotor cortex and bimanual training. Brain Res. 1618: 61-74, 2015. https://doi.org/10.1016/j.brainres.2015.05.028

Newsome WT and Paré EB. A selective impairment of motion perception following lesions of the middle temporal visual area (mt). J. Neurosci. 8: 2201-2211, 1988. https://doi.org/10.1523/JNEUROSCI.08-06-02201.1988

Nunez PL. A method to estimate local skull resistance in living subjects. IEEE Trans. Biomed. Eng. 902-904, 1987. https://doi.org/10.1109/TBME.1987.326104

Nunez PL, Srinivasan R, Westdorp AF, Wijesinghe RS, Tucker DM, Silberstein RB and Cadusch PJ. Eeg coherency: I: Statistics, reference electrode, volume conduction, laplacians, cortical imaging, and interpretation at multiple scales. Electroencephalogr. Clin. Neurophysiol. 103: 499-515, 1997. https://doi.org/10.1016/S0013-4694(97)00066-7

Oldfield RC. The assessment and analysis of handedness: The edinburgh inventory. Neuropsychologia 9: 97-113, 1971. https://doi.org/10.1016/0028-3932(71)90067-4

Pelt SV, Heil L, Kwisthout J, Ondobaka S, Rooij IV and Bekkering H. Beta- and gamma-band activity reflect predictive coding in the processing of causal events. Soc. Cogn. Affect. Neurosci. 11: nsw017, 2016. https://doi.org/10.1093/scan/nsw017

Perrin F, Pernier J, Bertrand O and Echallier J. Spherical splines for scalp potential and current density mapping. Electroencephalogr. Clin. Neurophysiol. 72: 184-187, 1989. https://doi.org/10.1016/0013-4694(89)90180-6

668 Pfurtscheller G and Lopes dS, F. H. Event-related eeg/meg synchronization and desynchronization:
669 Basic principles. Clin. Neurophysiol. 110: 1842-1857, 1999.
670 https://doi.org/10.1016/S1388-2457(99)00141-8
671 Rey HG, Fried I and Quiroga RQ. Timing of single-neuron and local field potential responses in the
672 human medial temporal lobe. Curr. Biol. 24: 299-304, 2014.
673 https://doi.org/10.1016/j.cub.2013.12.004
674 Rubinov M and Sporns O. Complex network measures of brain connectivity: Uses and
675 interpretations. NeuroImage 52: 1059-1069, 2010. https://doi.org/10.1016/j.neuroimage.2009.10.003
676 Seidler RD, Bloomberg JJ and Stelmach GE. Context-dependent arm pointing adaptation. Behav.
677 Brain Res. 119: 155-166, 2001. https://doi.org/10.1016/S0166-4328(00)00347-8
678 Shafer RL, Solomon EM, Newell KM, Lewis MH and Bodfish JW. Visual feedback during motor
679 performance is associated with increased complexity and adaptability of motor and neural output.
680 Behav. Brain Res. 376: 112214, 2019. https://doi.org/10.1016/j.bbr.2019.112214
681 Smits-Engelsman BC, Van Galen GP and Duysens J. Force levels in uni-and bimanual isometric
682 tasks affect variability measures differently throughout lifespan. Motor Control 8: 437-449, 2004.
683 https://doi.org/10.1123/mcj.8.4.437
684 Sosnoff JJ and Newell KM. Intermittent visual information and the multiple time scales of visual
685 motor control of continuous isometric force production. Percept. Psychophys. 67: 335-344, 2005.
686 https://doi.org/10.3758/BF03206496
687 Stanley ML, Simpson SL, Dagenbach D, Lyday RG, Burdette JH and Laurienti PJ. Changes in brain
688 network efficiency and working memory performance in aging. PLoS One 10: e0123950, 2015.
689 https://doi.org/10.1371/journal.pone.0123950

690 Tracy BL and Enoka RM. Older adults are less steady during submaximal isometric contractions
691 with the knee extensor muscles. J. Appl. Physiol. 92: 1004-1012, 2002.
692 https://doi.org/10.1152/japplphysiol.00954.2001
693 Tuladhar AM, Huurne Nt, Schoffelen JM, Maris E, Oostenveld R and Jensen O. Parieto-occipital
694 sources account for the increase in alpha activity with working memory load. Hum. Brain Mapp. 28:
695 785-792, 2007. https://doi.org/10.1002/hbm.20306
696 Ushiyama J, Yamada J, Liu M and Ushiba J. Individual difference in β-band corticomuscular
697 coherence and its relation to force steadiness during isometric voluntary ankle dorsiflexion in healthy
698 humans. Clin. Neurophysiol. 128: 303-311, 2017. https://doi.org/10.1016/j.clinph.2016.11.025
699 Wang L, Metzak PD, Honer WG and Woodward TS. Impaired efficiency of functional networks
700 underlying episodic memory-for-context in schizophrenia. J. Neurosci. 30: 13171-13179, 2010.
701 https://doi.org/10.1523/JNEUROSCI.3514-10.2010
702 Wang Q, Su TP, Zhou Y, Chou KH, Chen IY, Jiang T and Lin CP. Anatomical insights into disrupted
703 small-world networks in schizophrenia. NeuroImage 59: 1085-1093, 2012.
704 https://doi.org/10.1016/j.neuroimage.2011.09.035
705 Wang WE, Roy A, Misra G, Archer DB, Ribeiro-Dasilva MC, Fillingim RB and Coombes SA.
706 Motor-evoked pain increases force variability in chronic jaw pain. J. Pain 19: 636-648, 2018.
707 https://doi.org/10.1016/j.jpain.2018.01.013
708 Yordanova J, Falkenstein M and Kolev V. Aging-related changes in motor response-related theta
709 activity. Int. J. Psychophysiol. 2020. https://doi.org/10.1016/j.ijpsycho.2020.03.005
710 Yu Q, Sui J, Rachakonda S, He H, Pearlson G and Calhoun VD. Altered small-world brain networks
711 in temporal lobe in patients with schizophrenia performing an auditory oddball task. Front. Syst.

712 Neurosci. 5: 7, 2011. https://doi.org/10.3389/fnsys.2011.00007

713 Zarka D, Cevallos C, Petieau M, Hoellinger T, Dan B and Cheron G. Neural rhythmic symphony of
714 human walking observation: Upside-down and uncoordinated condition on cortical theta, alpha, beta
715 and gamma oscillations. Front. Syst. Neurosci. 8: 169, 2014.
716 https://doi.org/10.3389/fnsys.2014.00169

717

718

719

720

721

722

723

724

725

726

727

728

729

730

731

732

733 **Figures:**

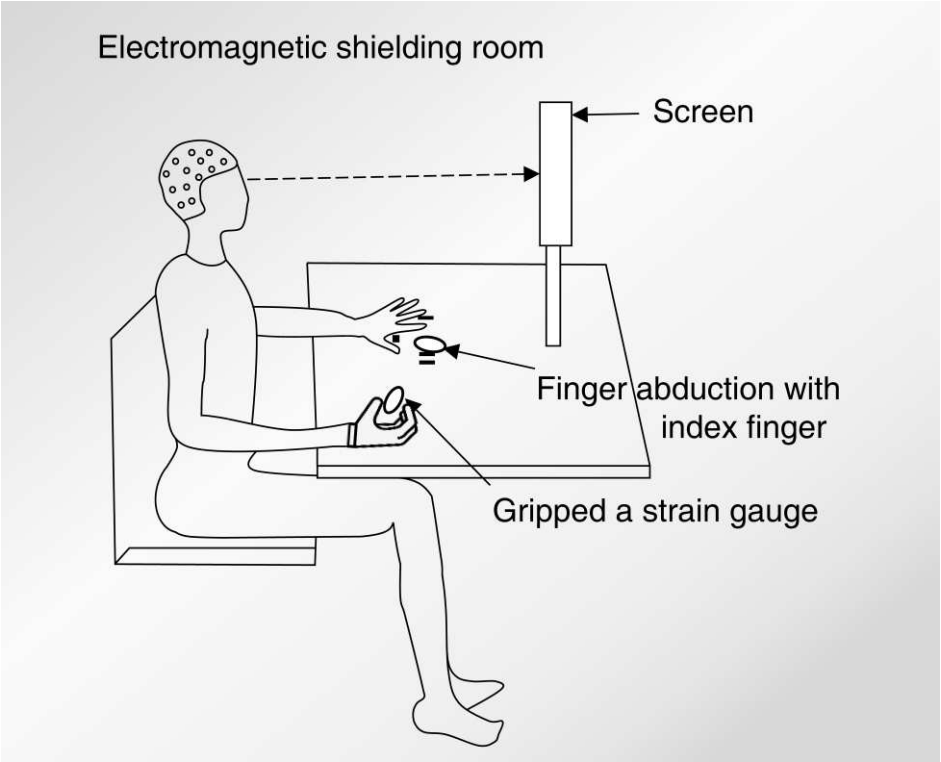

734

735 **Figure 1**. Experimental setup and visual feedback task on computer screen. Participants sat in an electromagnetic
736 shielding room, approximately 100cm in front of the monitor. The subjects had to perform precise unimanual and
737 bimanual hand movements according to the experimental orders. Right hand gripped a strain gauge to output a 2-N
738 constant force with index finger and the thumb. The subjects were instructed to abduct the index of their left hand
739 to exert two types of force involving 5% MVC and 50% MVC by squeezing a strain gauge.

740

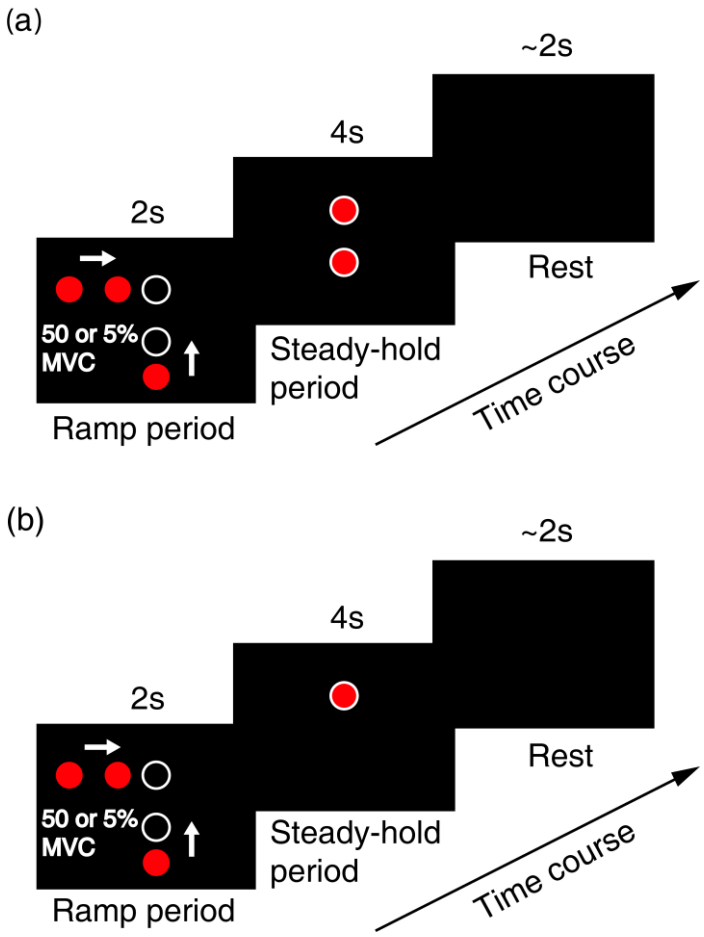

741

742 **Figure 2.** The schematic of experiment process and the visual feedback on the screen. Each trail contained 6s, the
743 subjects adjusted the exerted force to target force in the first two seconds, then maintained the target force for the
744 last 4s. Next, subjects rested for 2s. The solid circle was the exerted force, the hollow ring represent the target force.
745 The horizontal and vertical circle were controlled by the left hand and right hand respectively. The distance
746 between horizontal circle and ring was determined by the target force corresponding to 5% MVC and 50% MVC.
747 The pair of vertical circle and ring disappeared in the steady-hold periods. Unimanual task contained 60 trials and
748 bimanual task contained 40 trials. (a) Bimanual tasks with visual feedback on right hand during steady-hold period.
749 (b) Bimanual tasks without visual feedback on right hand during steady-hold period.

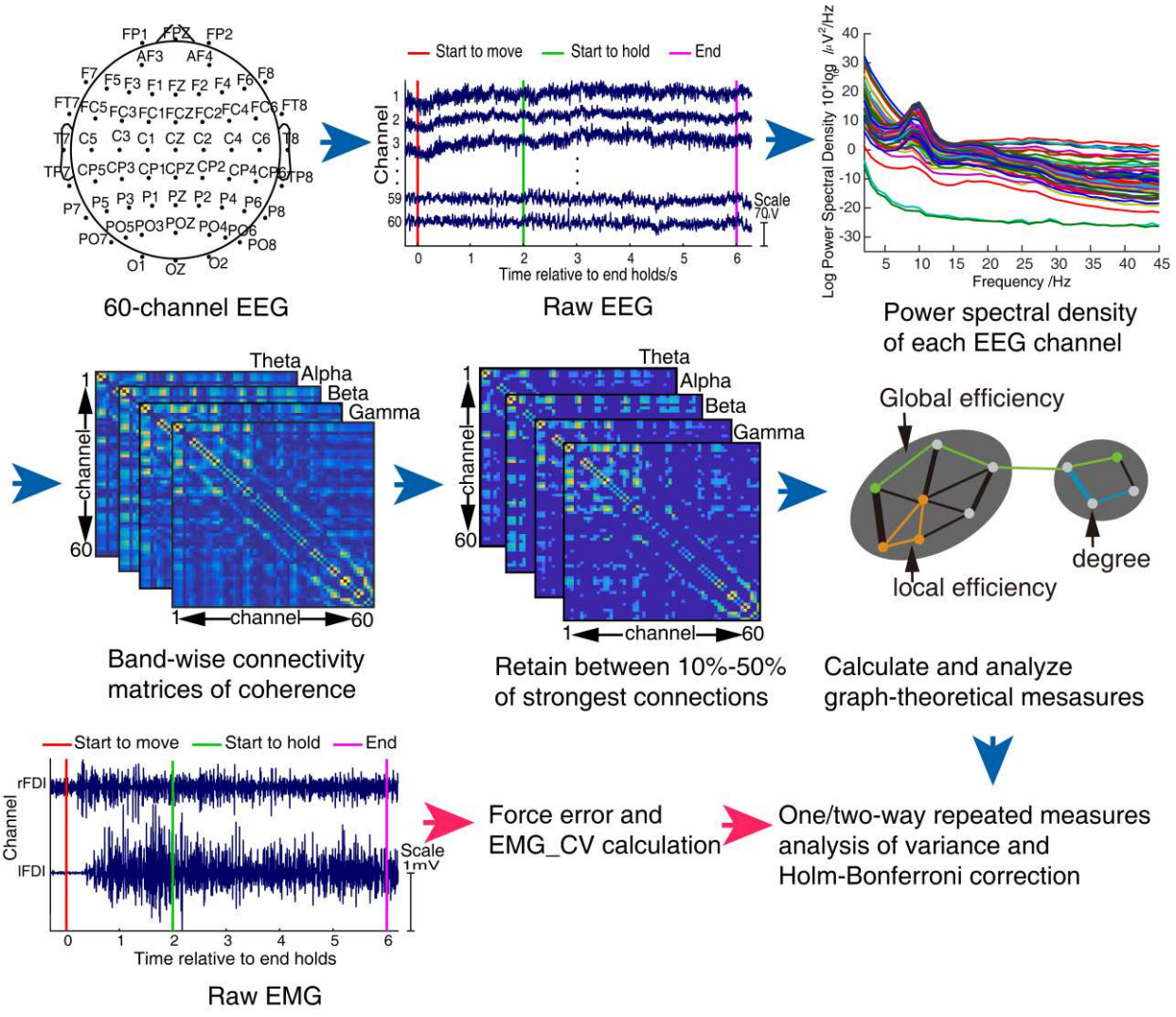

Figure 3. The flowchart of the data analysis

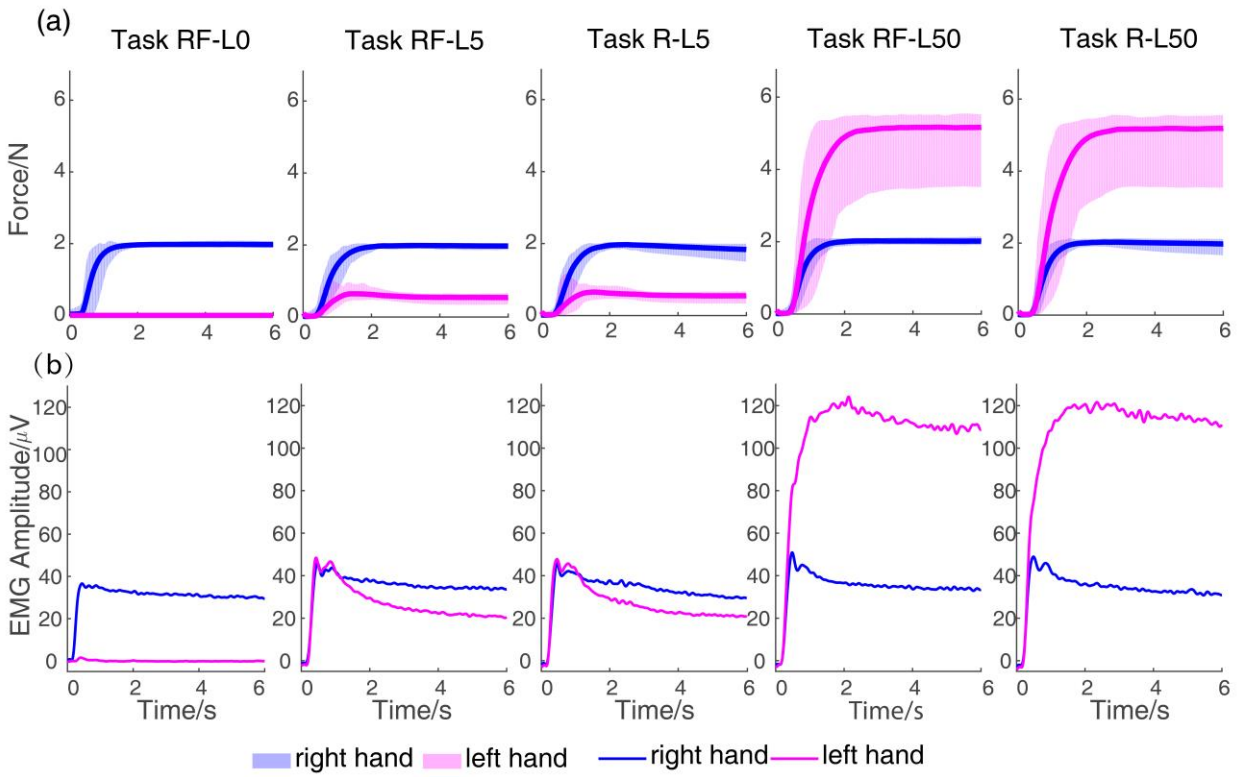

Figure 4. Average time courses of behavior across all subjects for each task during ramp-hold period. Blue line means exerted force/EMG activities of right hand. Magenta line means exerted force/EMG activities of left hand. (a) Average forces of both hands for each condition. The x-axis depicts time during movement. The y-axis denotes the values of the force. Shaded areas represented the exerted force across the all subjects. (b) Average EMG activities of both hands for each condition. The x-axis depicts time during movement. The y-axis denotes the values of the EMG activities.

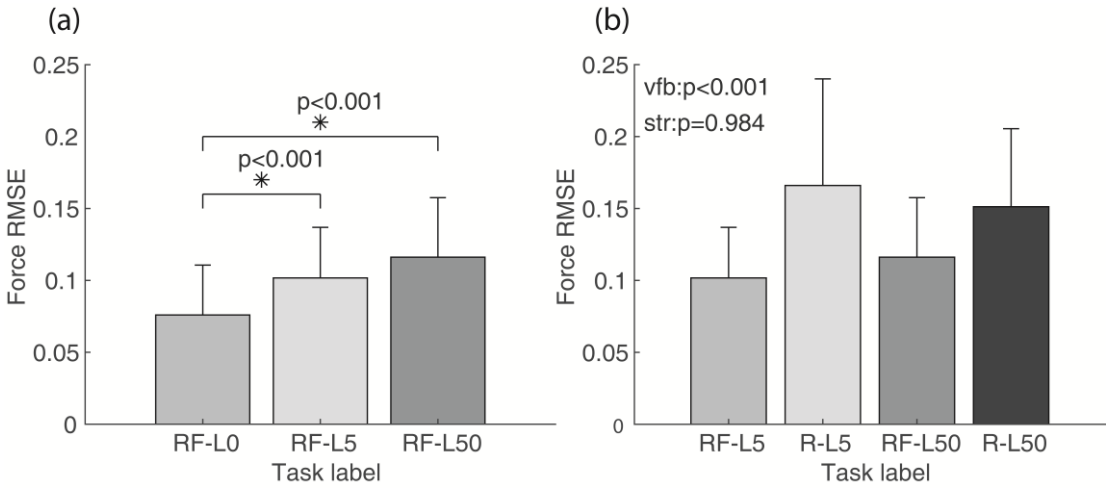

Figure 5. Average force RMSE and the results of statistical analysis for each task. The x-axis depicts each task across all the subjects. The y-axis denotes the values of force RMSE. Error bar means standard error (N=21). (a) The mean force RMSE for tasks RF-L0, RF-L5 and RF-L50. (b) The mean force RMSE for tasks RF-L5, R-L5, RF-L50 and R-L50. * refers to p<0.05 with Holm–Bonferroni correction for post hoc test, vfb means visual feedback for right hand, str means strength level of left hand.

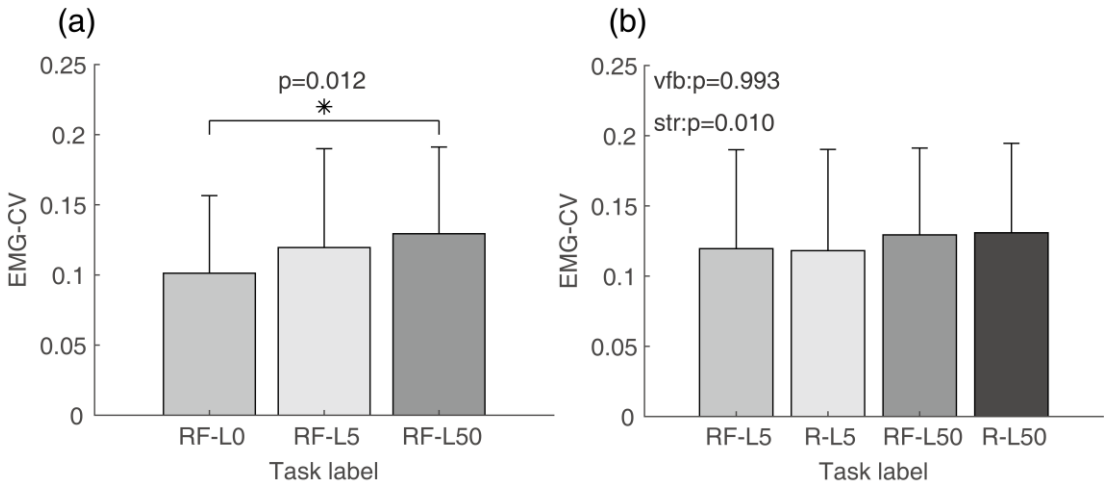

774

775 **Figure 6**. Average EMG_CV and the results of statistical analysis for each task across all the subjects. The x-axis

776 depicts each task across all the subjects. The y-axis denotes the values of the EMG_CV. Error bar means standard

777 error (*N*=21). (a) The mean EMG_CV for tasks RF-L0, RF-L5 and RF-L50. (b) The mean EMG_CV for tasks

778 RF-L5, R-L5, RF-L50 and R-L50, vfb means visual feedback for right hand, str means strength level of left hand.

779

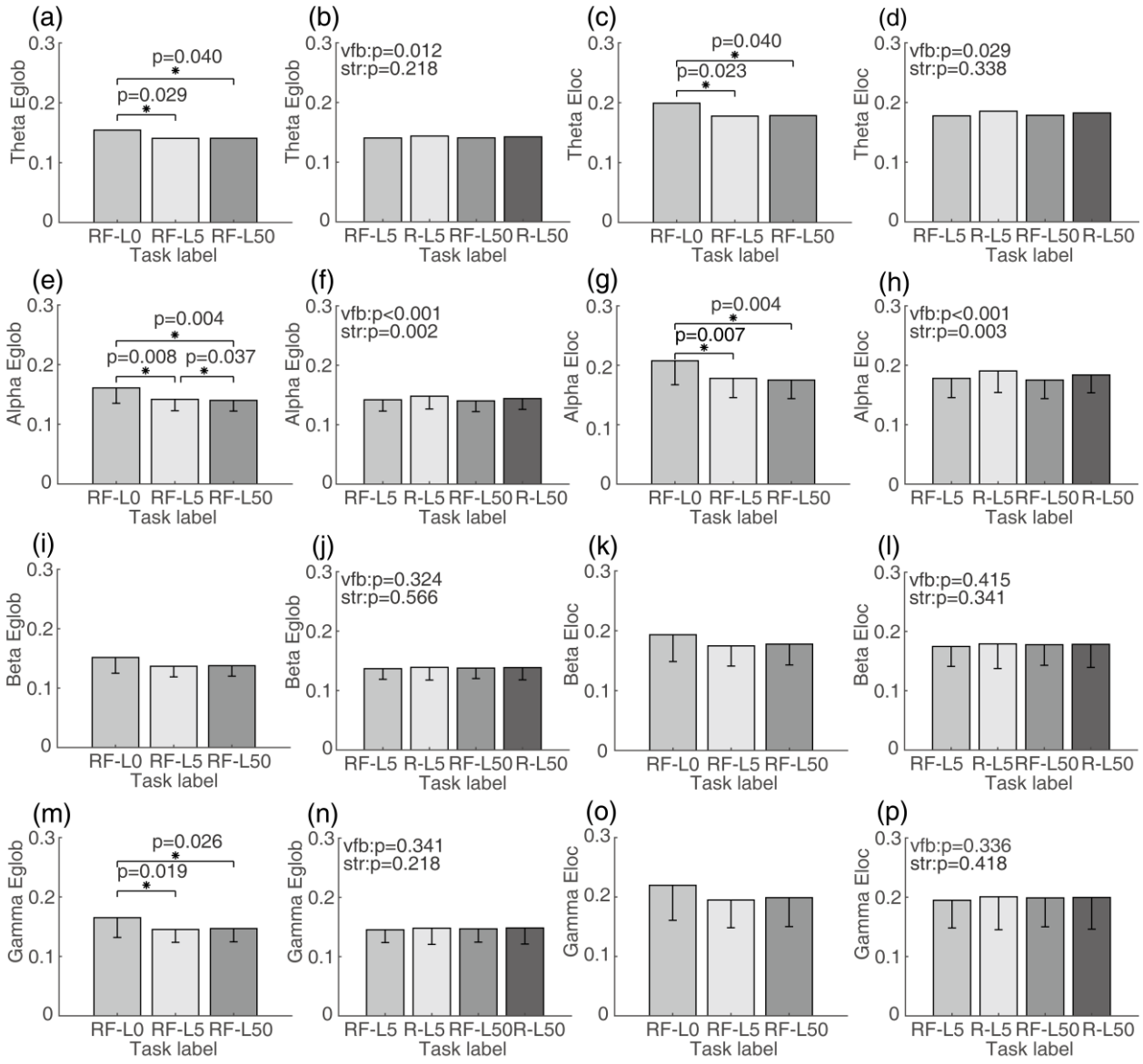

Figure 7. Average global efficiency and local efficiency in different band and the results of statistical analysis for each task. The x-axis depicts each task across all the subjects. The y-axis denotes the values of the global or local efficiency. Error bar means standard error (N=21). * refers to p<0.05 with Holm–Bonferroni correction for post hoc test. vfb means visual feedback for right hand, str means strength level of left hand. (a) The mean global efficiency in the theta band for tasks RF-L0, RF-L5 and RF-L50. (b) The mean global efficiency in the theta band for tasks RF-L5, R-L5, RF-L50 and R-L50. (c) The mean local efficiency in the theta band for tasks RF-L0, RF-L5 and RF-L50. (d) The mean local efficiency in the theta band for tasks RF-L5, R-L5, RF-L50 and R-L50. (e) The mean global efficiency in the alpha band for tasks RF-L0, RF-L5 and RF-L50. (f) The mean global efficiency in the alpha

band for tasks RF-L5, R-L5, RF-L50 and R-L50. (g) The mean local efficiency in the alpha band for tasks RF-L0, RF-L5 and RF-L50. (h) The mean local efficiency in the alpha band for tasks RF-L5, R-L5, RF-L50 and R-L50. (i) The mean global efficiency in the beta band for tasks RF-L0, RF-L5 and RF-L50. (j) The mean global efficiency in the beta band for tasks RF-L5, R-L5, RF-L50 and R-L50. (k) The mean local efficiency in the beta band for tasks RF-L0, RF-L5 and RF-L50. (l) The mean local efficiency in the beta band for tasks RF-L5, R-L5, RF-L50 and R-L50. (m) The mean global efficiency in the gamma band for tasks RF-L0, RF-L5 and RF-L50. (n) The mean global efficiency in the gamma band for tasks RF-L5, R-L5, RF-L50 and R-L50. (o) The mean local efficiency in the gamma band for tasks RF-L0, RF-L5 and RF-L50. (p) The mean local efficiency in the gamma band for tasks RF-L5, R-L5, RF-L50 and R-L50.

Figures

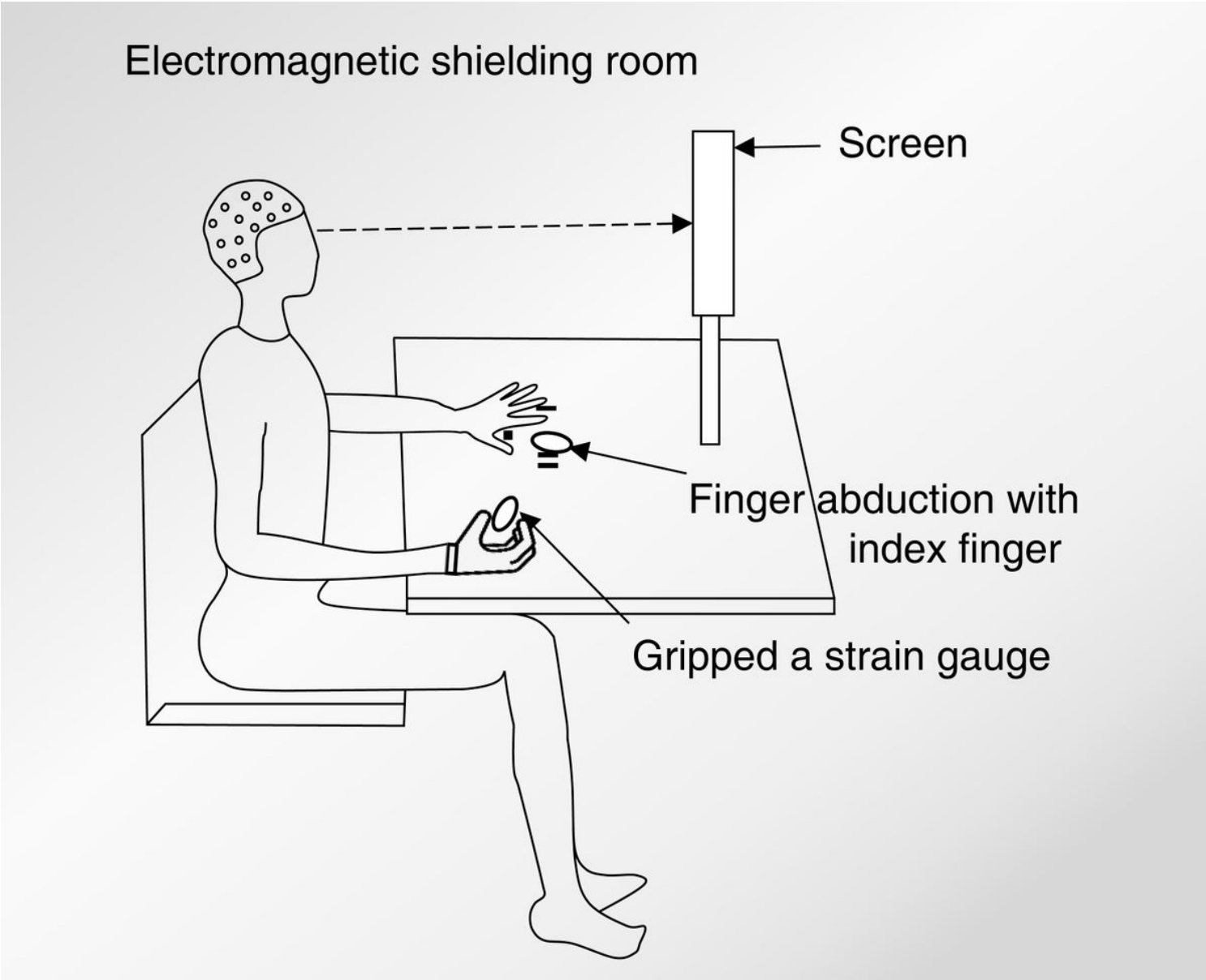

Figure 1

Experimental setup and visual feedback task on computer screen. Participants sat in an electromagnetic shielding room, approximately 100cm in front of the monitor. The subjects had to perform precise unimanual and bimanual hand movements according to the experimental orders. Right hand gripped a strain gauge to output a 2-N constant force with index finger and the thumb. The subjects were instructed to abduct the index of their left hand to exert two types of force involving 5% MVC and 50% MVC by squeezing a strain gauge.

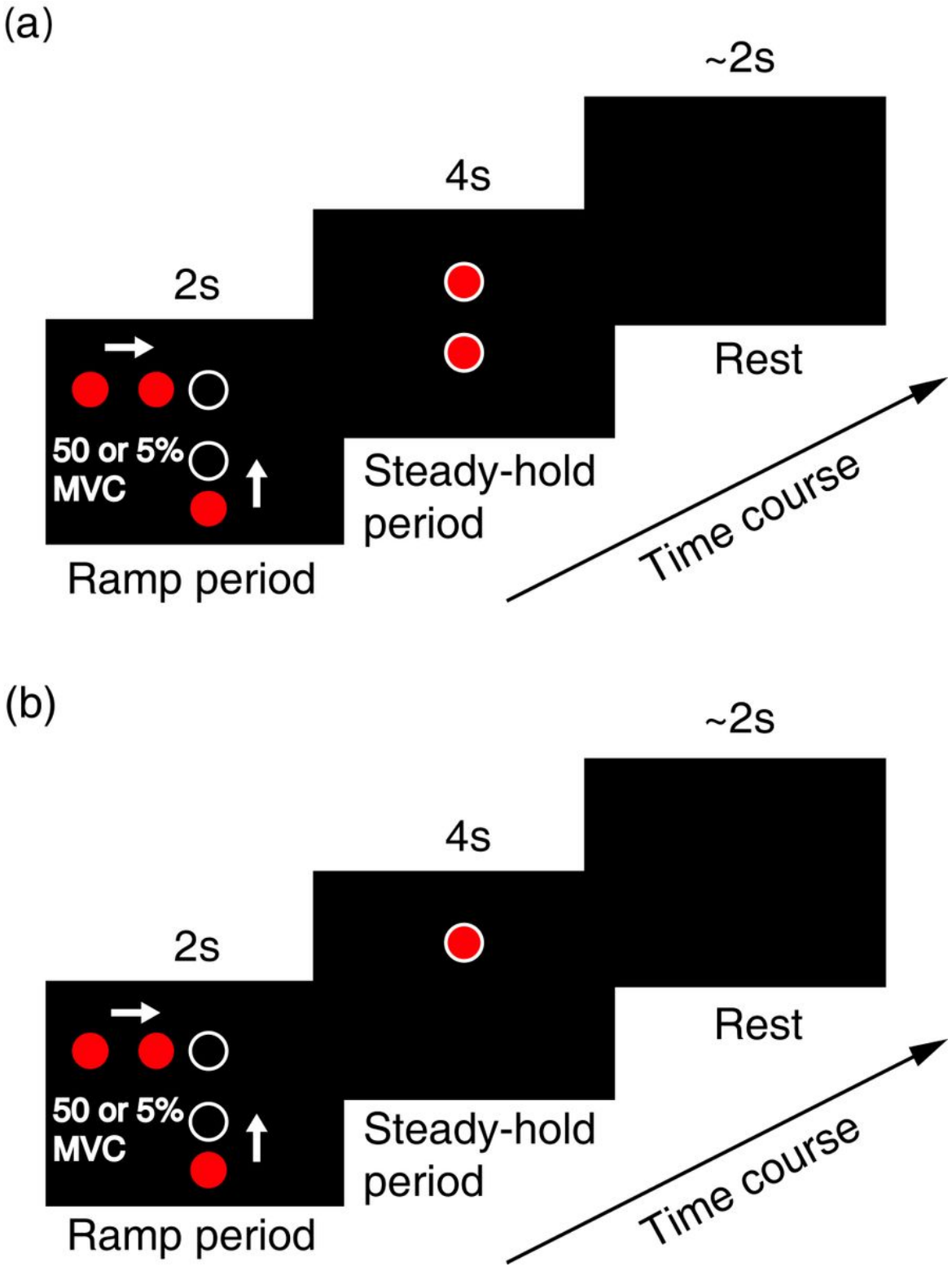

Figure 2

The schematic of experiment process and the visual feedback on the screen. Each trail contained 6s, the subjects adjusted the exerted force to target force in the first two seconds, then maintained the target force for the last 4s. Next, subjects rested for 2s. The solid circle was the exerted force, the hollow ring represent the target force. The horizontal and vertical circle were controlled by the left hand and right hand respectively. The distance between horizontal circle and ring was determined by the target force

corresponding to 5% MVC and 50% MVC. The pair of vertical circle and ring disappeared in the steady-hold periods. Unimanual task contained 60 trials and bimanual task contained 40 trials. (a) Bimanual tasks with visual feedback on right hand during steady-hold period. (b) Bimanual tasks without visual feedback on right hand during steady-hold period.

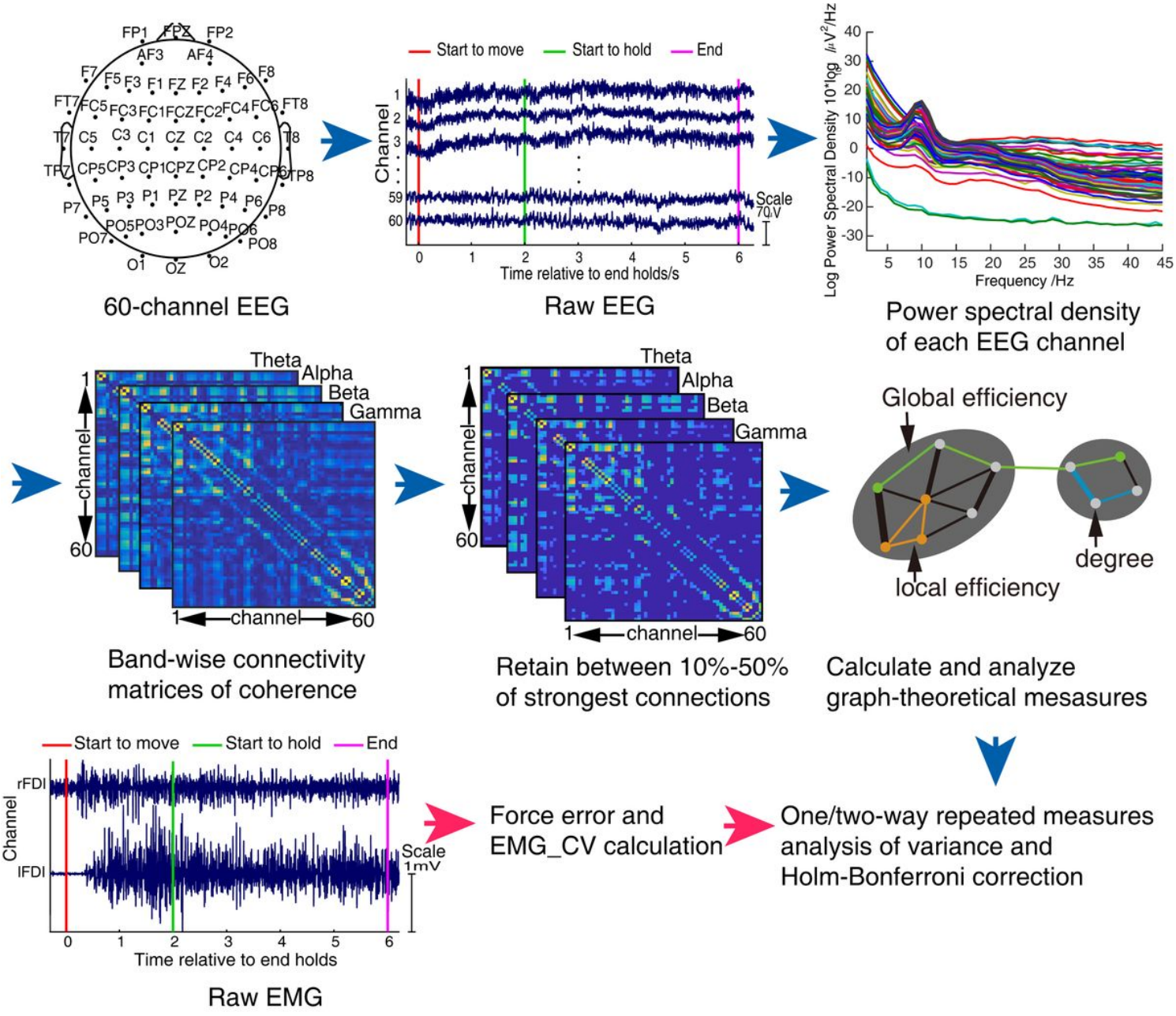

Figure 3

The flowchart of the data analysis

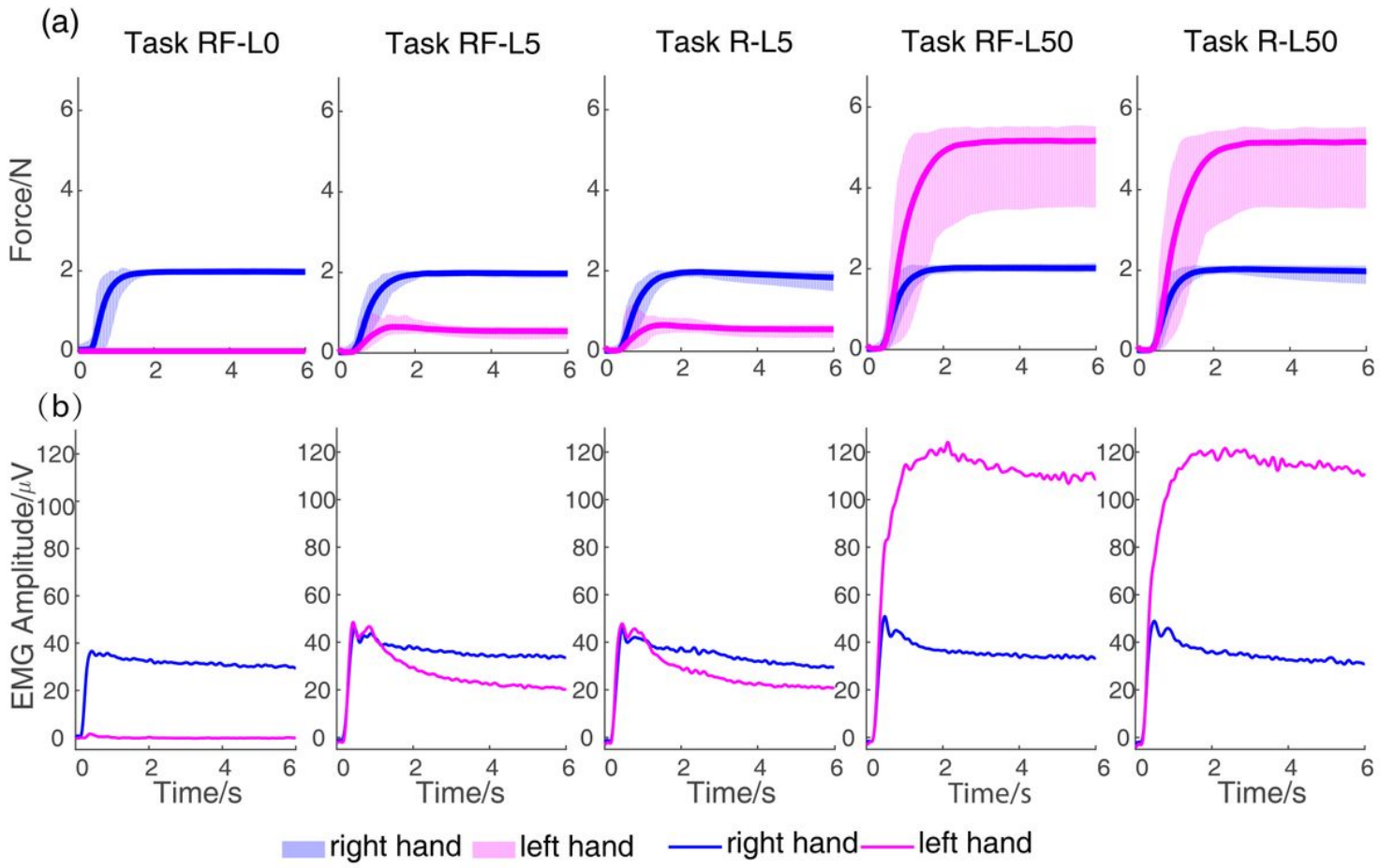

Figure 4

Average time courses of behavior across all subjects for each task during ramp-hold period. Blue line means exerted force/EMG activities of right hand. Magenta line means exerted force/EMG activities of left hand. (a) Average forces of both hands for each condition. The x-axis depicts time during movement. The y-axis denotes the values of the force. Shaded areas represented the exerted force across the all subjects. (b) Average EMG activities of both hands for each condition. The x-axis depicts time during movement. The y-axis denotes the values of the EMG activities.

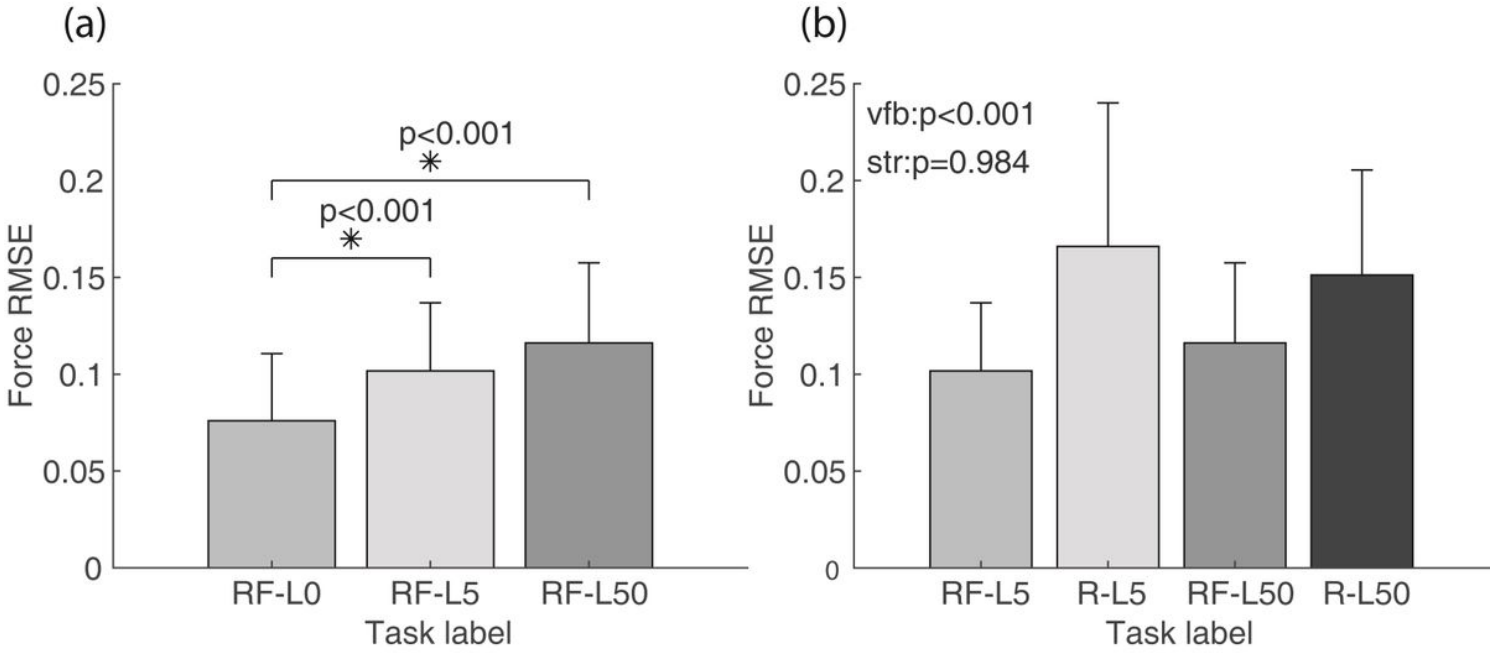

Figure 5

Average force RMSE and the results of statistical analysis for each task. The x-axis depicts each task across all the subjects. The y-axis denotes the values of force RMSE. Error bar means standard error (N=21). (a) The mean force RMSE for tasks RF-L0, RF-L5 and RF-L50. (b) The mean force RMSE for tasks RF-L5, R-L5, RF-L50 and R-L50. * refers to p<0.05 with Holm–Bonferroni correction for post hoc test, vfb means visual feedback for right hand, str means strength level of left hand.

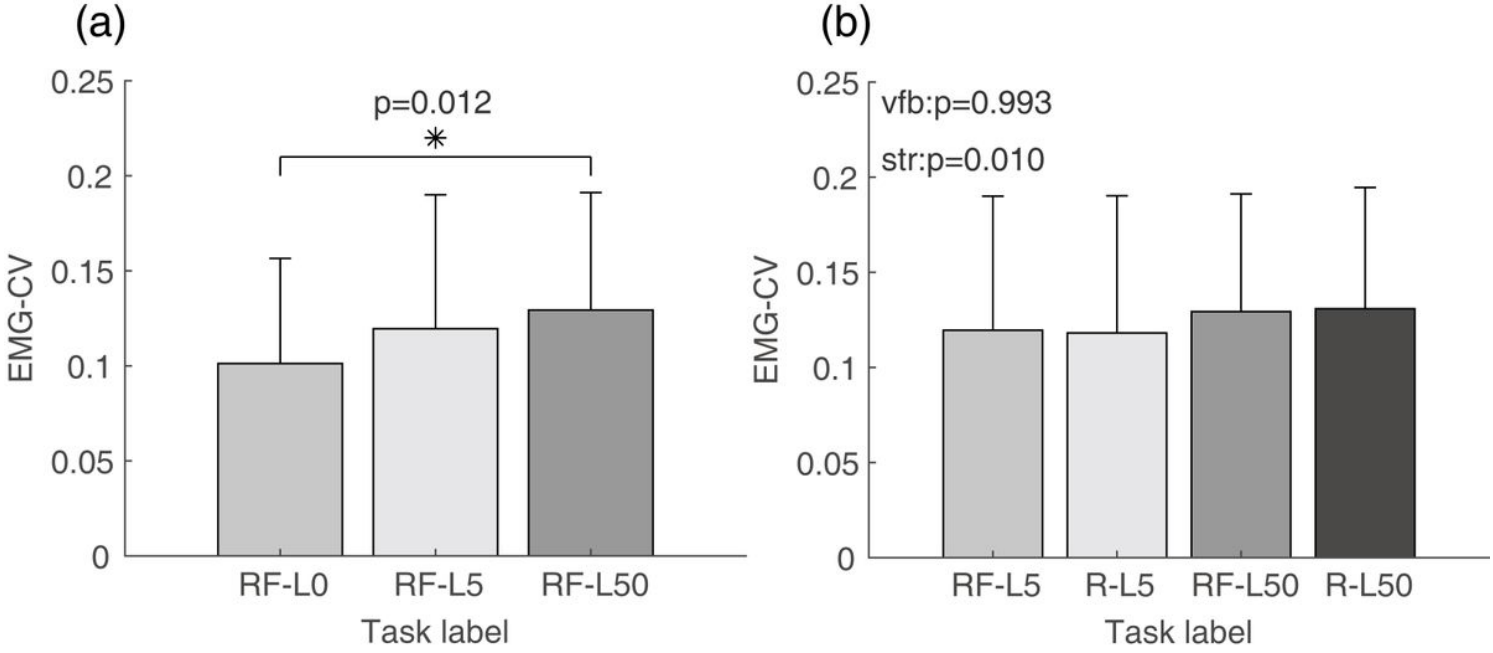

Figure 6

Average EMG_CV and the results of statistical analysis for each task across all the subjects. The x-axis depicts each task across all the subjects. The y-axis denotes the values of the EMG_CV. Error bar means

standard error (N=21). (a) The mean EMG_CV for tasks RF-L0, RF-L5 and RF-L50. (b) The mean EMG_CV for tasks RF-L5, R-L5, RF-L50 and R-L50, vfb means visual feedback for right hand, str means strength level of left hand.

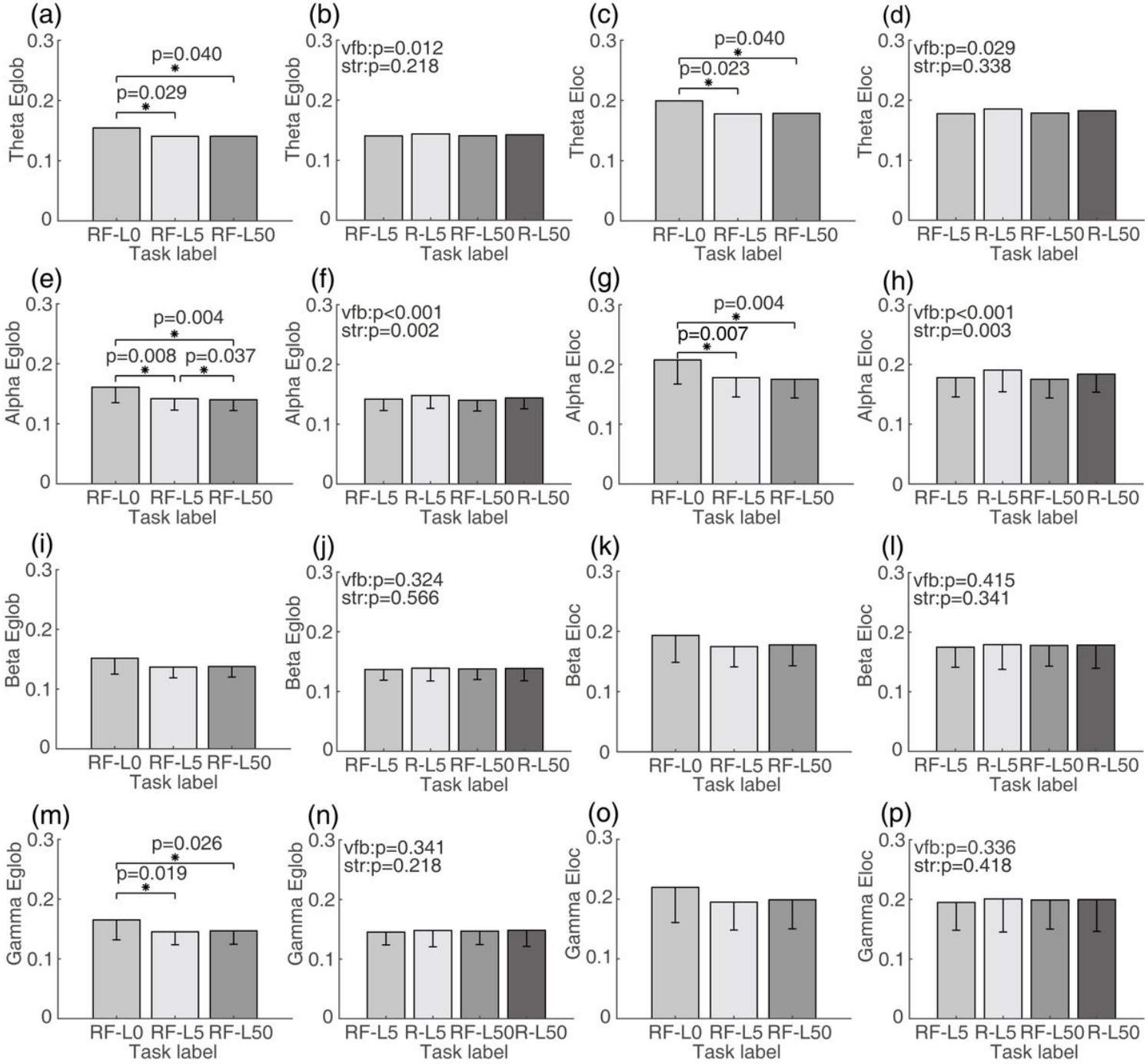

Figure 7

Average global efficiency and local efficiency in different band and the results of statistical analysis for each task. The x-axis depicts each task across all the subjects. The y-axis denotes the values of the global or local efficiency. Error bar means standard error (N=21). * refers to p<0.05 with Holm–Bonferroni correction for post hoc test. vfb means visual feedback for right hand, str means strength level of left hand. (a) The mean global efficiency in the theta band for tasks RF-L0, RF-L5 and RF-L50. (b) The mean

global efficiency in the theta band for tasks RF-L5, R-L5, RF-L50 and R-L50. (c) The mean local efficiency in the theta band for tasks RF-L0, RF-L5 and RF-L50. (d) The mean local efficiency in the theta band for tasks RF-L5, R-L5, RF-L50 and R-L50. (e) The mean global efficiency in the alpha band for tasks RF-L0, RF-L5 and RF-L50. (f) The mean global efficiency in the alpha band for tasks RF-L5, R-L5, RF-L50 and R-L50. (g) The mean local efficiency in the alpha band for tasks RF-L0, RF-L5 and RF-L50. (h) The mean local efficiency in the alpha band for tasks RF-L5, R-L5, RF-L50 and R-L50. (i) The mean global efficiency in the beta band for tasks RF-L0, RF-L5 and RF-L50. (j) The mean global efficiency in the beta band for tasks RF-L5, R-L5, RF-L50 and R-L50. (k) The mean local efficiency in the beta band for tasks RF-L0, RF-L5 and RF-L50. (l) The mean local efficiency in the beta band for tasks RF-L5, R-L5, RF-L50 and R-L50. (m) The mean global efficiency in the gamma band for tasks RF-L0, RF-L5 and RF-L50. (n) The mean global efficiency in the gamma band for tasks RF-L5, R-L5, RF-L50 and R-L50. (o) The mean local efficiency in the gamma band for tasks RF-L0, RF-L5 and RF-L50. (p) The mean local efficiency in the gamma band for tasks RF-L5, R-L5, RF-L50 and R-L50.